How to make a good SAXS data treatment ? Yes we can !

O. TACHE, O. SPALLA

Emplacement logotypes financeurs/partenaires

> **But why the local contact ask me that ?**

A anonymous student

Recommandations for setting Up a SAXS Experiment and obtain high-quality and meaningful data

Experiment Objectives:
What do you want to learn about your sample? Is it particle size, shape, distribution, concentration, or other structural properties?

Instrument Selection:
Select the appropriate SAXS instrument based on your experimental objectives. (q- ranges wavelength), which affect the size of the structures you can probe.

Instrument Calibration:
Ensure that the SAXS instrument is properly calibrated.

Sample Preparation :

Sample Type: Sample preparation varies depending on the sample type.
Sample Concentration: The optimal sample concentration depends on the sample's scattering power and the sensitivity of the instrument. Too high a concentration can cause multiple scattering effects, while too low a concentration can result in a weak signal.
Sample Holder:** Choose a sample holder that is appropriate for your sample type and experimental conditions. Sample holders are available for capillaries, paste cells, solids, and powders.
Sample Thickness: Sample thickness should be optimized to minimize X-ray absorption while maximizing the scattering signal. The optimal thickness depends on the linear absorption coefficient of the sample and the X-ray wavelength.
Matrix/Solvent Preparation: If the sample is dispersed in a matrix or solvent : It is important to choose a solvent that:
* Stably disperses the analyte
* Has a scattering cross section that is significantly different from that of the analyte
* Can suspend a sufficient concentration of the analyte
* Is not too toxic or aggressive
- Does not absorb X-rays too much

Size Effects: : The intensity of the scattering signal is proportional to the sixth power of the particle size. Large particles dominate the signal and can obscure smaller particles.

Polydispersity : Size and form polydispersity complicate the saxs data treatment
●
Measurements and Data Analysis
Acquisition Time:
Choose an acquisition time long enough to obtain good counting statistics while minimizing potential damage to the sample. And optimizing the number of samples we can probe

Sample and Background Measurement:** Perform scattering measurements on the sample and a blank (matrix/solvent only). Background subtraction is essential to isolate the scattering signal from the particles.
Data Correction:** Apply corrections for instrumental effects, sample absorption, background, and detector efficiency

Summary

- SAXS/WAXS platform @CEA
- Safety
- Experiments Geometrical designs
  - Components
  - Measurement chain
- Data Treatment
- Images 2D
- IQ 1D Datas
- Metrology aspects

SAXS WAXS PLATFORM 2024 at CEA Saclay

2024 SWAXSlab

DOSIMETRY

Safety procedures

Safety procedures

Zone irradiante = zone rouge = zone infranchissable

Seules les personnes habilitées à effectuer les réglages peuvent utiliser les clés de dérogation permettant d'accéder en zone irradiante.

Pour des expériences de routine, le faisceau doit toujours être coupé lors des interventions autour des échantillons.

En cas de situation d'urgence, en référer au responsable ou utiliser les boutons d'arrêt d'urgence électrique.

En cas d'anomalie de fonctionnement ou sur les signalisations, en référer immédiatement au responsable de l'expérience.

Aucun étudiant ne peut utiliser les expériences en étant seul dans le laboratoire.

Notions de radioprotection

- pour le personnel classé B
  limite légale de débit de dose pour les extrémités : 150 mS /an
  limite légale de débit de dose pour l'organisme entier : 6 mS /an

- pour le personnel classé NE (non exposé)
  limite légale de débit de dose pour les extrémités : 50 mS /an
  limite légale de débit de dose pour l'organisme entier : 1 mS / an

50 mSv/an est la plus petite dose (de façon conservative) à partir de laquelle on ne peut prouver l'apparition de cancers (cette dose est aussi la radioactivité naturelle de plusieurs lieux sur Terre). Au delà de cette valeur, le nombre de cancers (mais pas de leur gravité) augmente avec la dose.

Dosimétrie

Mesuré : **8.3.10^{-8} mSv/photons** de 8 keV

SAXS
Débit de dose max dans le faisceau : avec 10.10^{7} ph/s -> 30 Sv/h soit 30 Gy/h **(faisceau 1x1 mm)**
(1Gy = 1Sv pour les rayons X)
Débit de dose à 10 cm en dehors du faisceau : 0.240 mSv/h
Débit de dose à l'extérieur de l'enceinte de protection : <1 µSv/h
Temps pour atteindre la limite légale dans le faisceau : 18 s
Temps pour atteindre la limite à 10 cm en dehors du faisceau : 300 h

XEUSS
Débit de dose max dans le faisceau : avec 2.5.10^{7} ph/s -> 7 Sv/h soit 7 Gy/h **(faisceau 1x1 mm)**
(1Gy = 1Sv pour les rayons X)

USAXS
Débit de dose max dans le faisceau : avec 4.10^{6} ph/s -> 1.2 Sv/h soit 1.2 Gy/h **(faisceau 10x1 mm)**
Temps pour atteindre la limite légale dans le faisceau : 451 s

ESRF ou SWING (faisceau de 10^{13} ph/s à 8 keV) -> 830 Sv/s

MOMAC (17 keV) :
Flux de 10^{8} photons/s
Avec **5.54.10^{-9} mSv/photons** de 17keV → Débit de dose max dans le faisceau : 2Sv/h 2Gy/h
Temps pour atteindre la limite légale dans le faisceau : 15 min

INSTRUMENTATION, Components of a SAXS instrument

Small Angles X-Ray Scattering (SAXS) :

- information on morphology of nanomaterials, size & polydispersity, volume, surface, form.
- dispersion state, concentration or particules agregation
- Large objects number
- in situ, non destructive, observation without sample modification

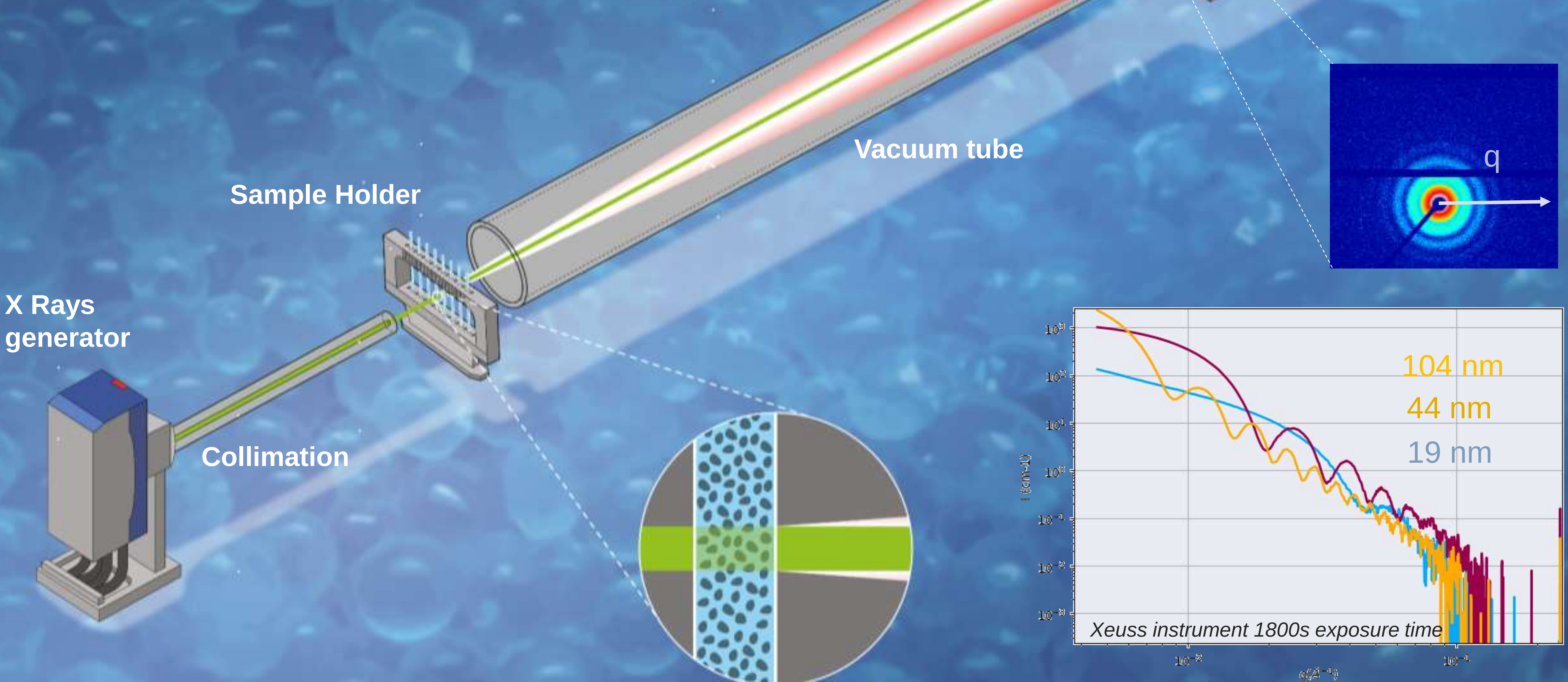

X-Rays production

Laboratory source

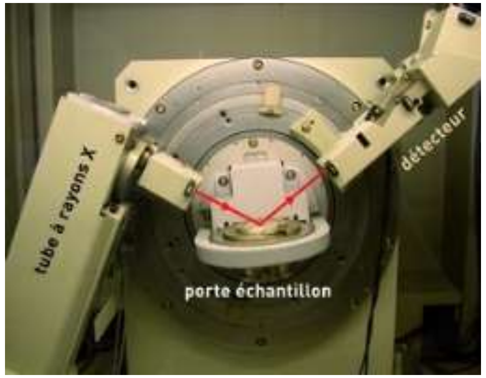

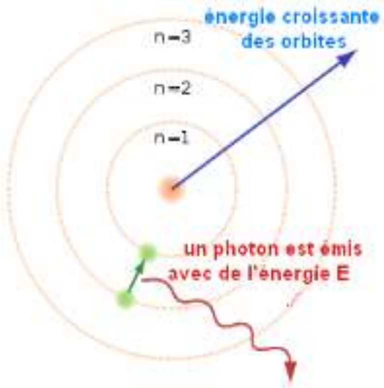

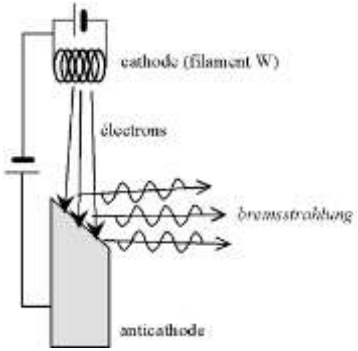

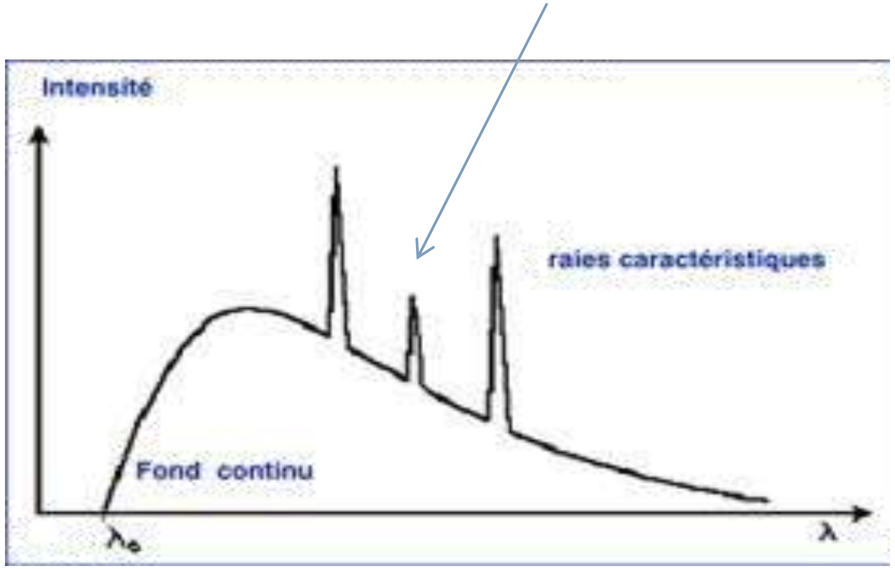

Synchrotron

Laboratory X-Rays Sources

Tubes

Large line and spot focus

Micro sources

spot focus *couplage avec optique*

Rotating Anode

Large line and spot focus High Flux (7x Micro source) (to be examined)

Metal Jet

Gallium (9.2 keV)

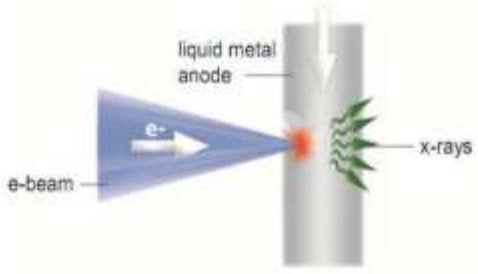

spot focus very High Flux (3X rotating anode)

monochromators

Perfect monochromator

The Bragg's Law for diffraction

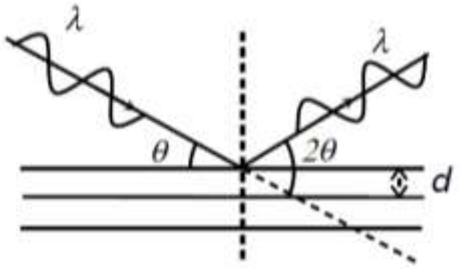

$$n\lambda = 2d \sin\theta$$

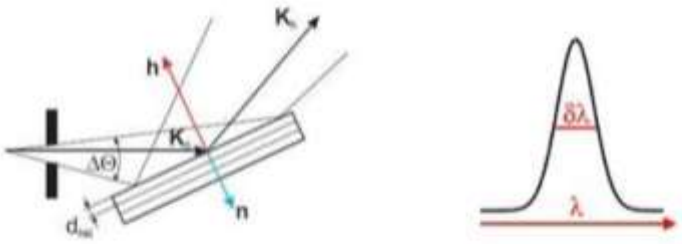

Effect of divergency in spectral purity

Monochromateur multicouche

Ellipsoid of revolution

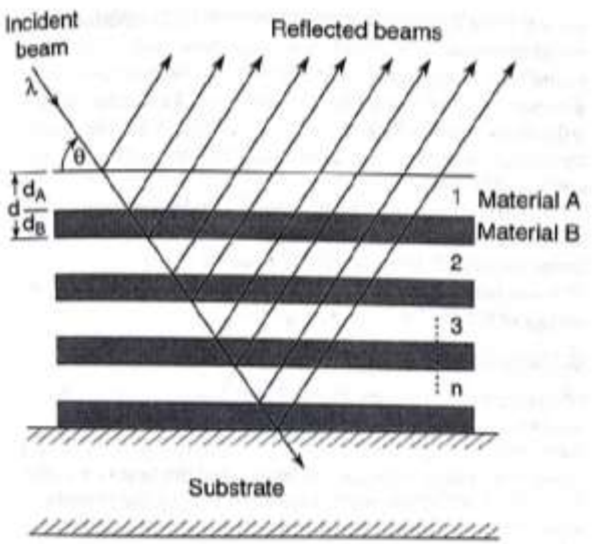

Very small reflection angle

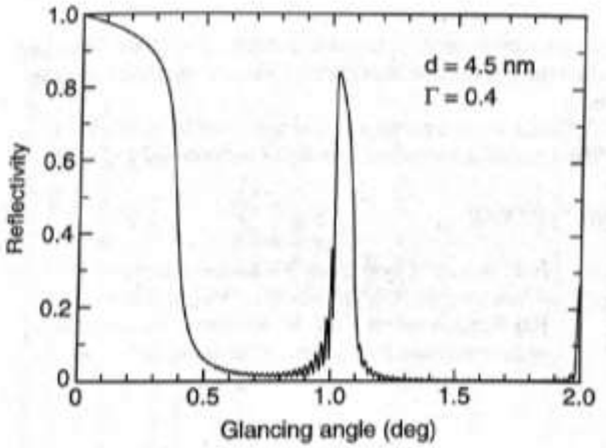

Collimation

➢ Increase the beam size

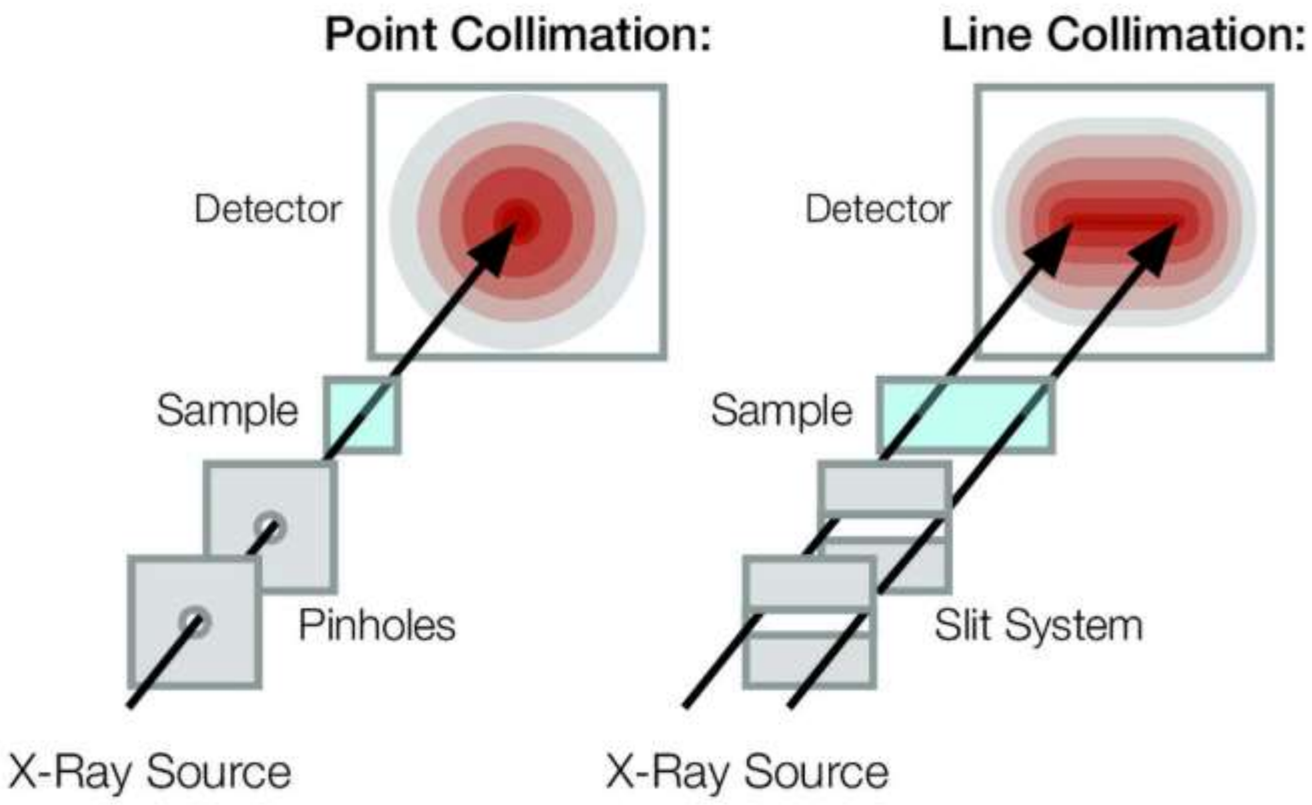

- Smaller beam, lower flux
+ no signal deformation

+ Higher flux
- Signal deformation, lower resolution, deconvolution

Kratky camera

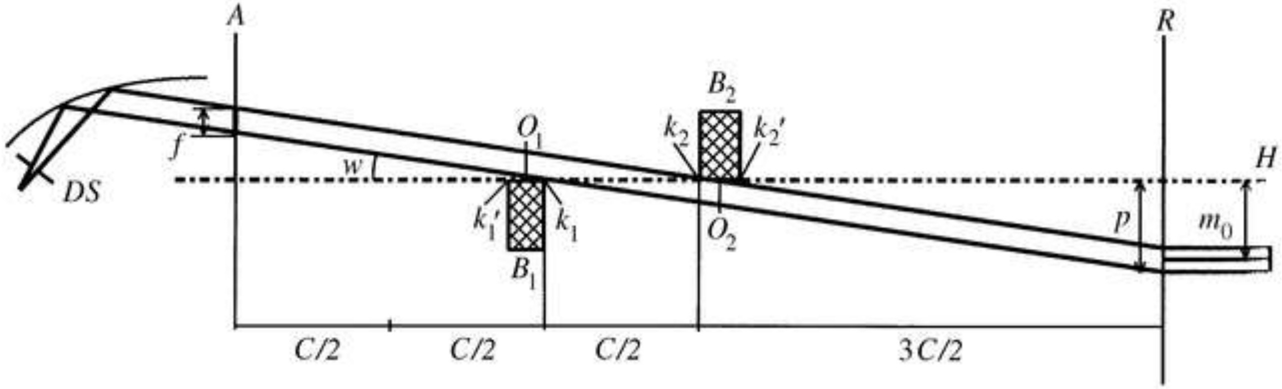

Rigaku

Anton Paar

Benefits:

- A compact system that delivers high flux on the sample
- Measure large q-space with a smaller, more affordable detector
- Truly parasitic scattering free, unlike pinhole systems that still retain some residual parasitic scattering
- Ideal for isotropic samples and GI SAXS
- High q resolution

From raw image to absolute intensity: Calibration of a Guinier-Mering camera with linear collimation

F. Né, I. Grillo, O. Taché et Th. Zemb

J. Phys. IV France **10** (2000)

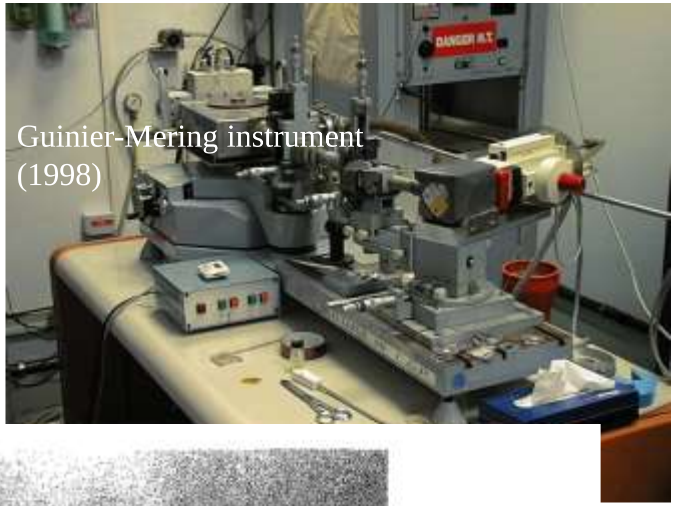

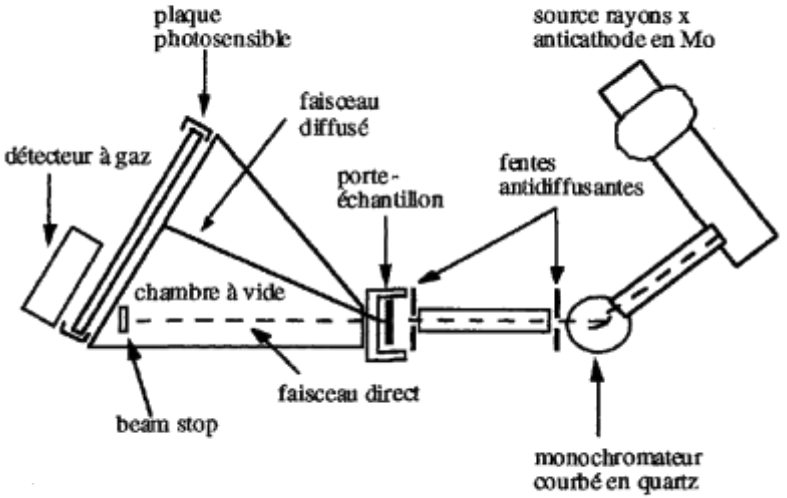

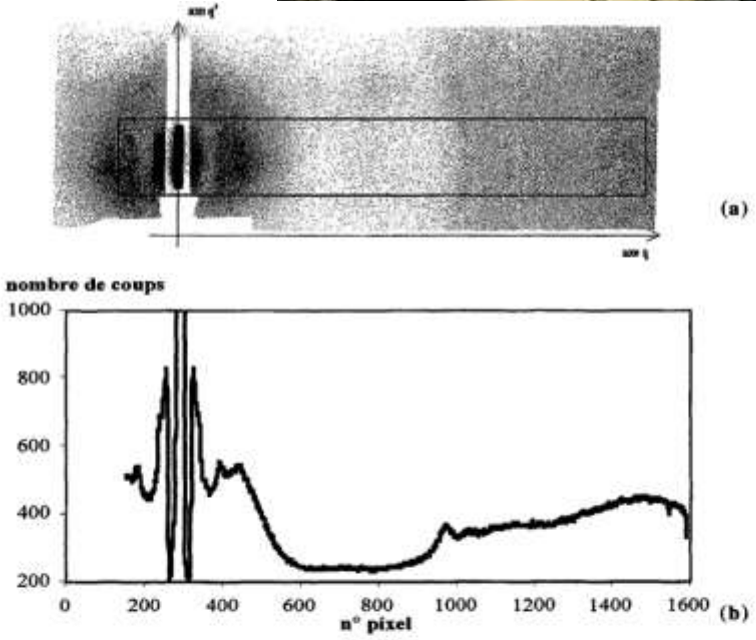

Figure 2 : (a) Image 2D d'un échantillon d'AOT, w=30% avec 1% de laponite, après une acquisition de 12 heures. (b) Le spectre brut (nombre de coups en fonction du n° du pixel) s'obtient par regroupement le long de l'axe q', dans un rectangle de la largeur du faisceau incident.

Figure 2 : (a) 2D scattering pattern from a lamellar sample of AOT (w=30%), with 1% of laponite clay particles after 12 hours exposure. (b) Raw spectrum (number of photons plotted against the pixel number) obtained by radial averaging the 2D picture along the q' axis, in a rectangle of the width of the direct beam.

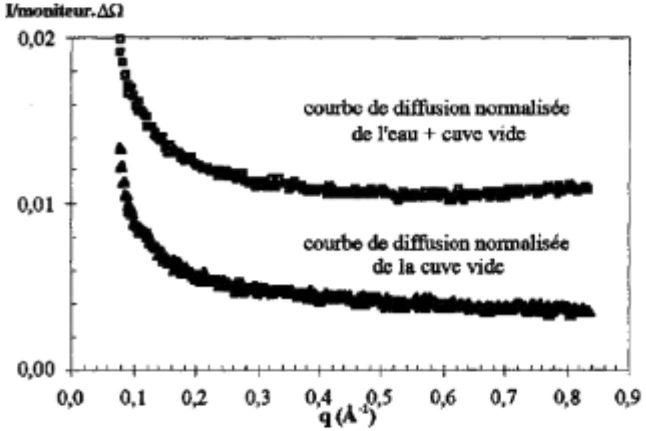

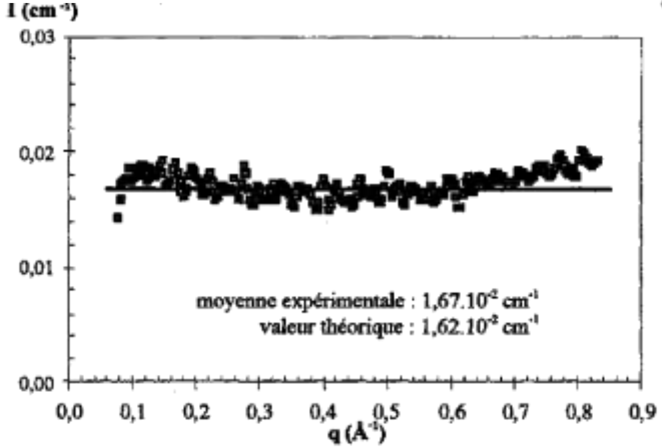

SAXS advantage at Mo (17 keV)

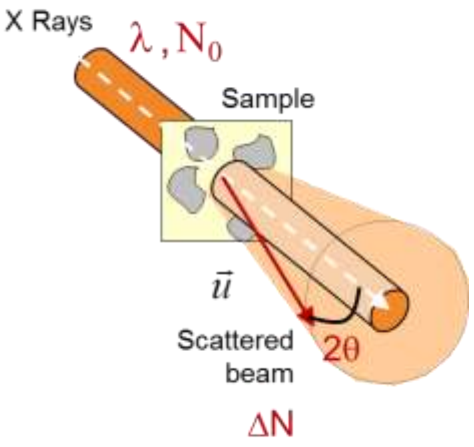

Incident Flux *Transmission* *Solid angle of the detector*

$$\Delta N = \Phi_0 \; S \; T \; p(\vec{u}) \, \Delta\Omega$$

Counts/s in the direction of the solid angle ΔΩ

Surface of the sample

$\Phi_0 \, S = N_0$

Probability of being Scattered in the direction u

Probability increases with thickness ***t***

$$p(\vec{u}) = t.\frac{d\Sigma}{d\Omega}$$

Intensive property of the material

$$\Delta N = N_0 . T.t . \frac{d\Sigma}{d\Omega}.\Delta\Omega$$

Need to be maximized, depends of the sample

ΔN ~ t T is maximum for t = 1/μ   and therefore T=1/t=0.37

H_2O	Cu K_{a1} 8.047 keV	ID02 ESRF 11.9 keV	Mo K_{a1} 17.48 keV
t Optimal	1.02 mm	2.96 mm	10.7 mm 3 mm
Transmission	0.34	0.34	0.71
T.t	0.34	1	**2.21**

x7

WAXS setup (2013 – 2023)

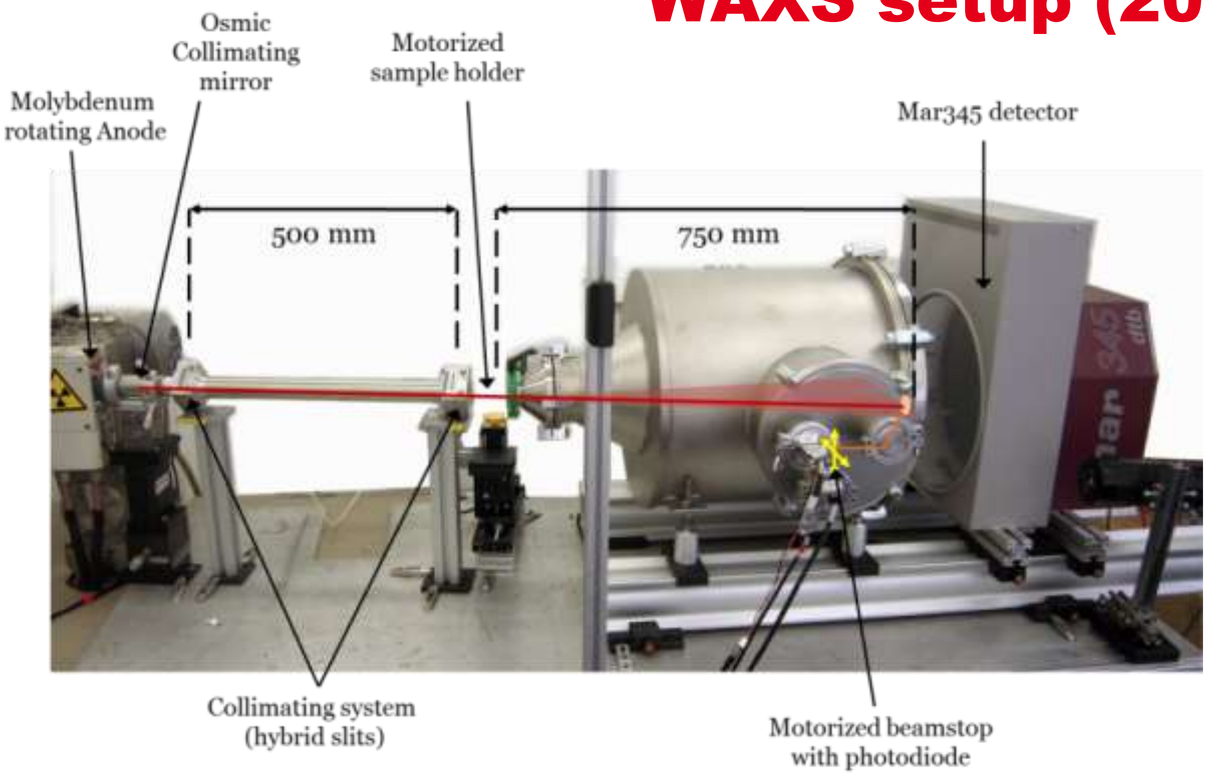

SAXS – WAXS (MOMAC)
q range : $4x10^{-2}$ to 4 A^{-1}
0.1 nm <-> 10 nm

λ=0.07 nm **E=17 keV (nanomaterials)**
Flux : 100 x 10^6 ph/s

MOMAC: a SAXS/WAXS laboratory instrument dedicated to nanomaterials.
O. Taché, and al
(2016). J. Appl. Cryst. 49

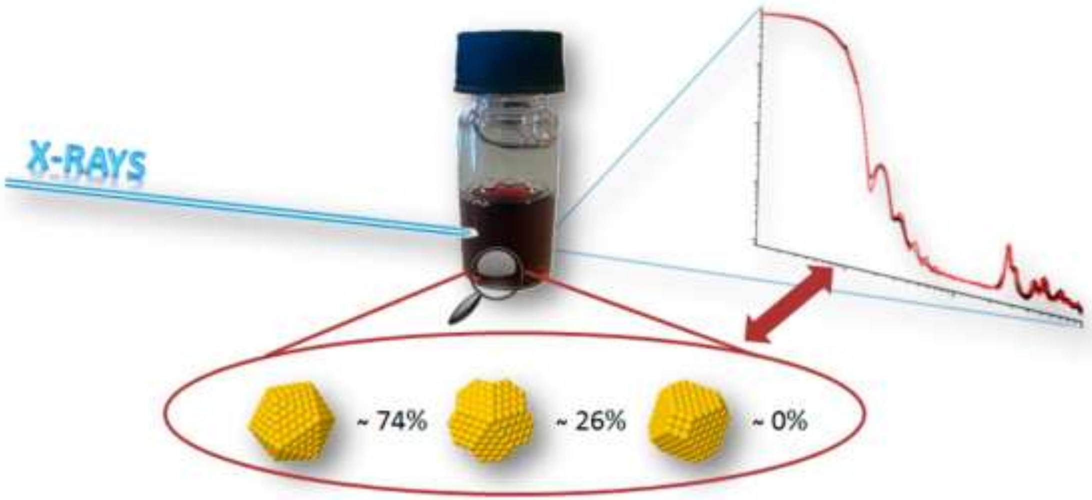

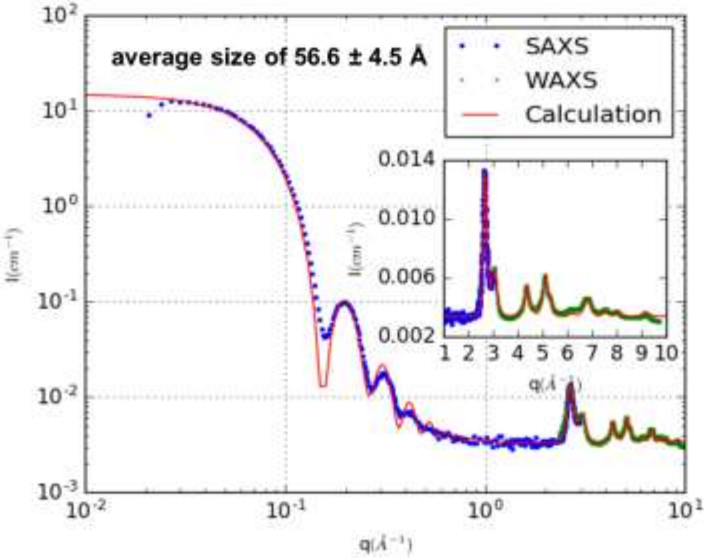

Blaise Fleury[*†]*, Robinson Cortes-Huerto*[†]*, Olivier Taché*[†]*, Fabienne Testard*[†]*, Nicolas Menguy*[‡]*, and Olivier Spalla*[†] *Nanoletter 2015*

USAXS - BONSE&HART GEOMETRY

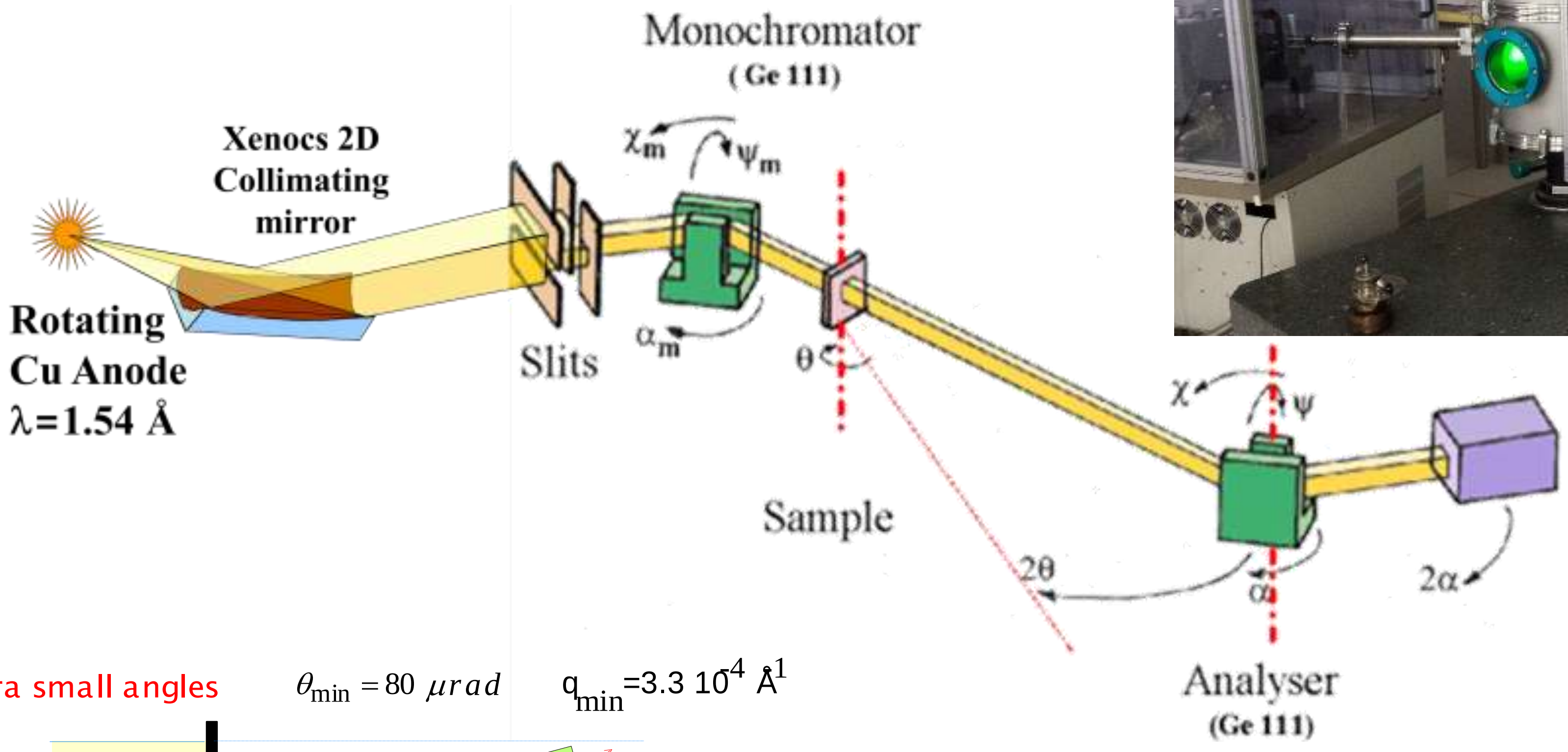

⇒Ultra small angles $\theta_{min} = 80\ \mu rad$ q_{min}=3.3 10^{-4} $Å^{-1}$

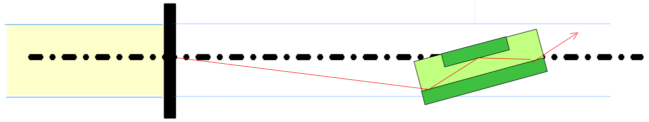

⇒ High resolution $\Delta\theta = 80\ \mu rad$ Δ q =3.10^{-4} $Å^{-1}$

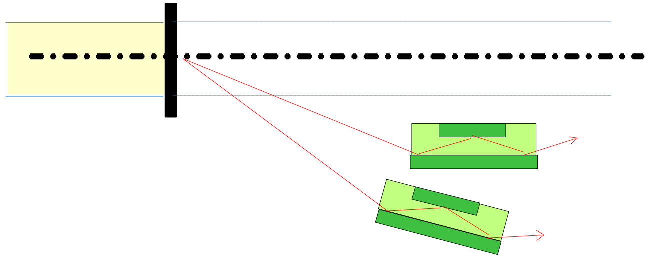

Parameters and performances	
λ	1.54 Å
beam size on sample H x V	3x11 mm^2
Channel cut crystals	Ge 111
Δq (FWHM)	3,14 10^{-4} $Å^{-1}$
q_{min} at 10^{-3} from maximum	4x10^{-4} $Å^{-1}$
q_{min} at 10^{-5} from maximum	2x10^{-3} $Å^{-1}$
Flux (with mirror)	7x10^{7} c/s
Divergence of incident beam H x V	80 µrad x 5mrad
Divergence of scattered beam H x V	80 µrad x 20mrad
q-range	2.10^{-4}<q<0.4 Å-1
d-range	3 µm <d< 15 Å

XEUSS 3 BH USAXS module

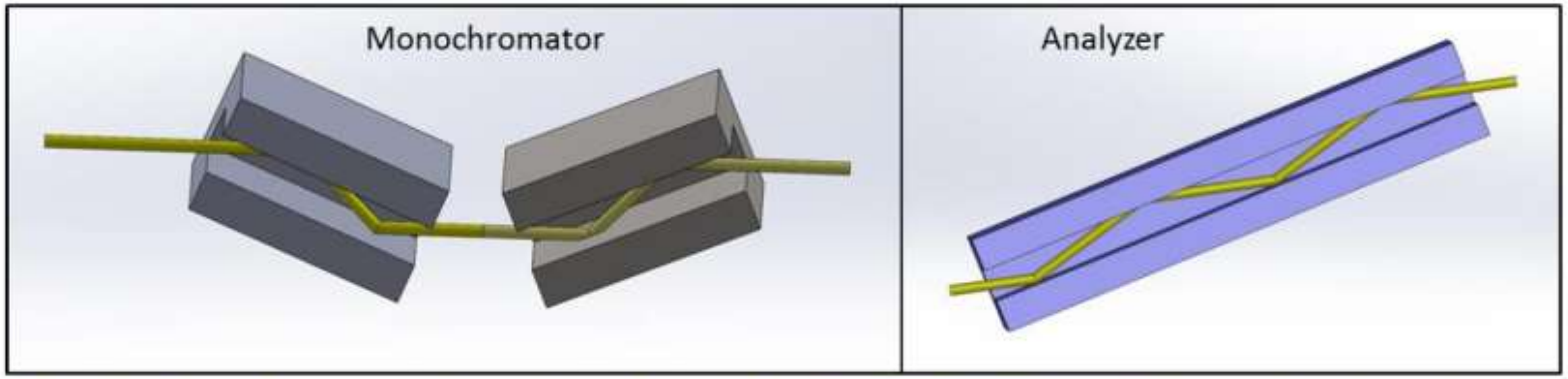

Figure 2 – Monochromator and analyzer schematics for the BH-USAXS. Multiple bounce (i.e channel-cut crystals) crystals reduce the scattering "tail" background. Please note the geometry of the monochromator assembly, divided into two separated crystals with two bounces each. This geometry assures a fix-exit effect on beam height.

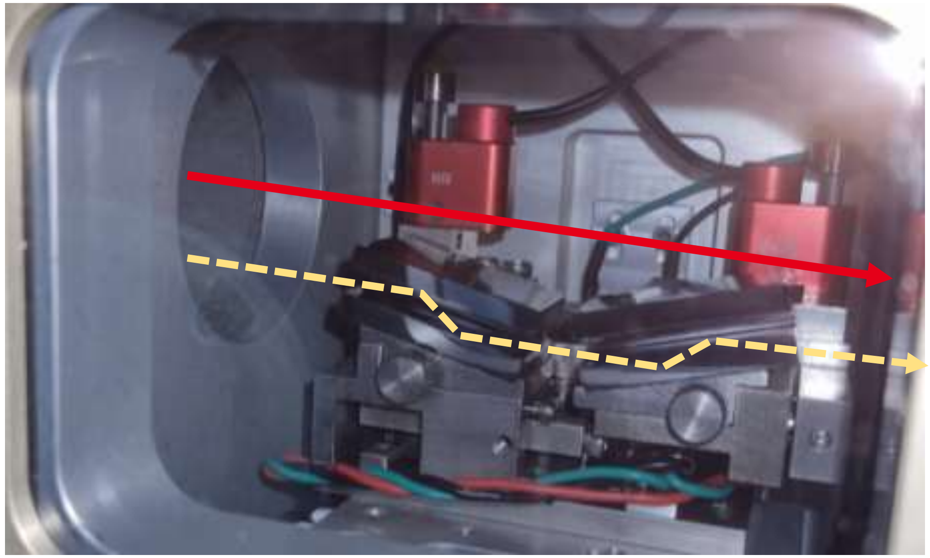

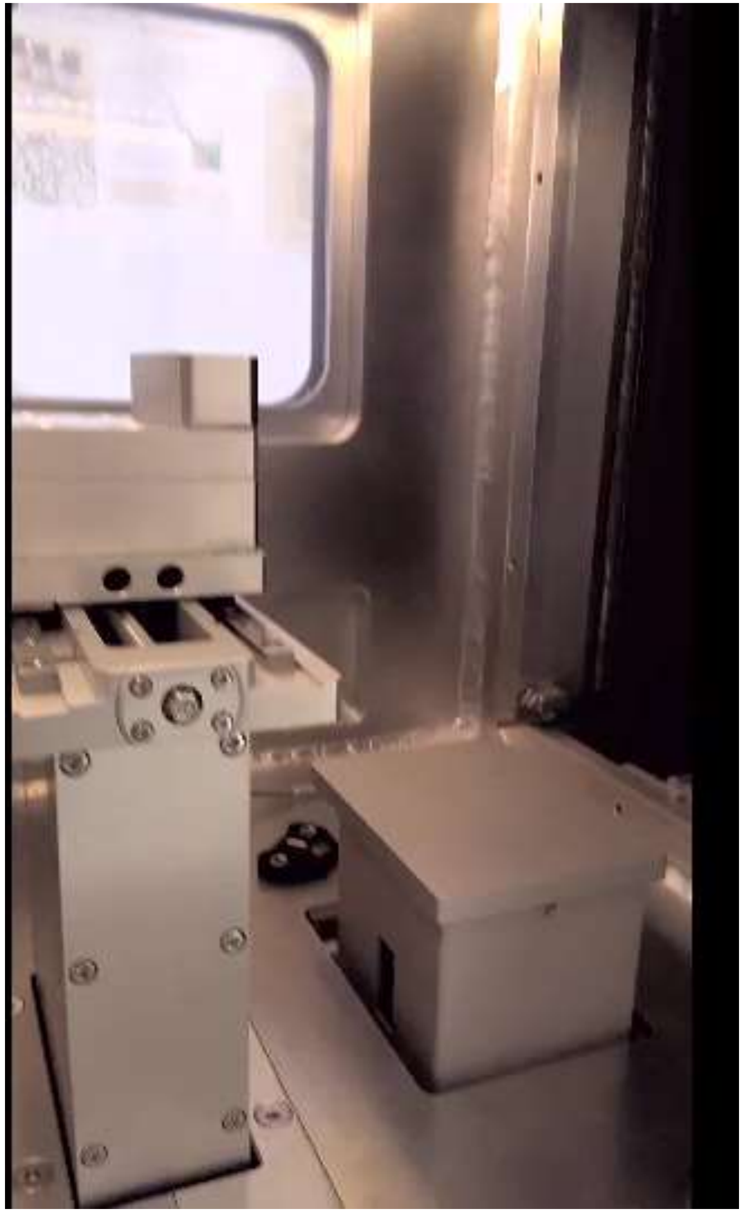

3 Pinholes geometry

➢ Increase beam size

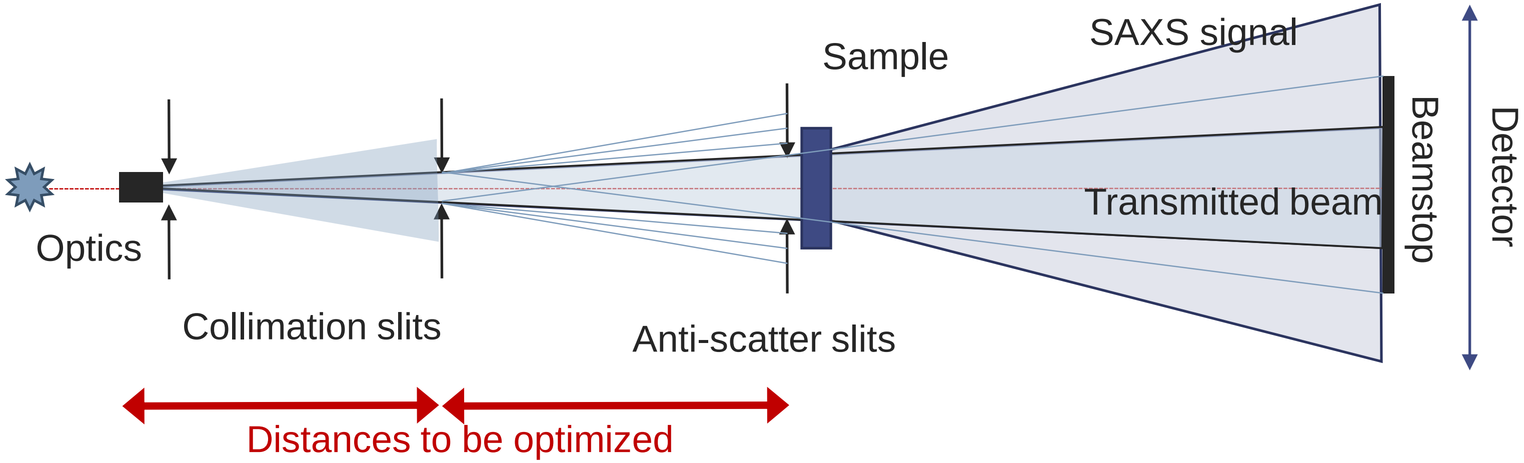

90 % x-rays provided by the source are lost

REVIEW OF SCIENTIFIC INSTRUMENTS VOLUME 74, NUMBER 4 APRIL 2003

Improving sensitivity of a small angle x-ray scattering camera with pinhole collimation using separated optical elements

Th. Zemb, O. Taché, F. Né, and O. Spalla[a]
Service de Chimie Moléculaire (D.R.E.C.A.M./C.E.A.), C.E./Saclay, F91191 Gif sur Yvette Cedex, France

Journal of
Applied
Crystallography
ISSN 0021-8898

A flux- and background-optimized version of the NanoSTAR small-angle X-ray scattering camera for solution scattering

Received 30 June 2003
Accepted 23 February 2004

Jan Skov Pedersen

Scatterless slits

<u>*Hybrid scatterless slits*</u>

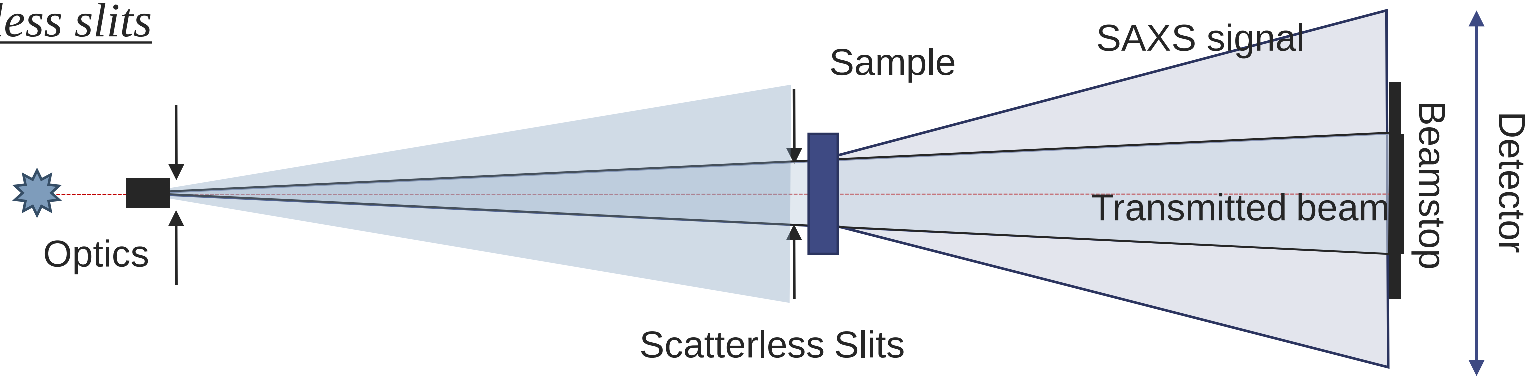

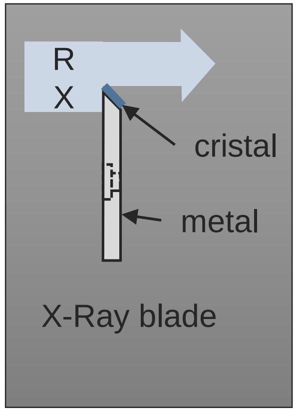

Youli Li and al,
Scatterless hybrid metal-single-crystal slit for small angle X-ray scattering and high-resolution X-ray diffraction
J. Appl. Cryst. (2008), **41**, 1134-1139

Scatterless slits : optimized setup

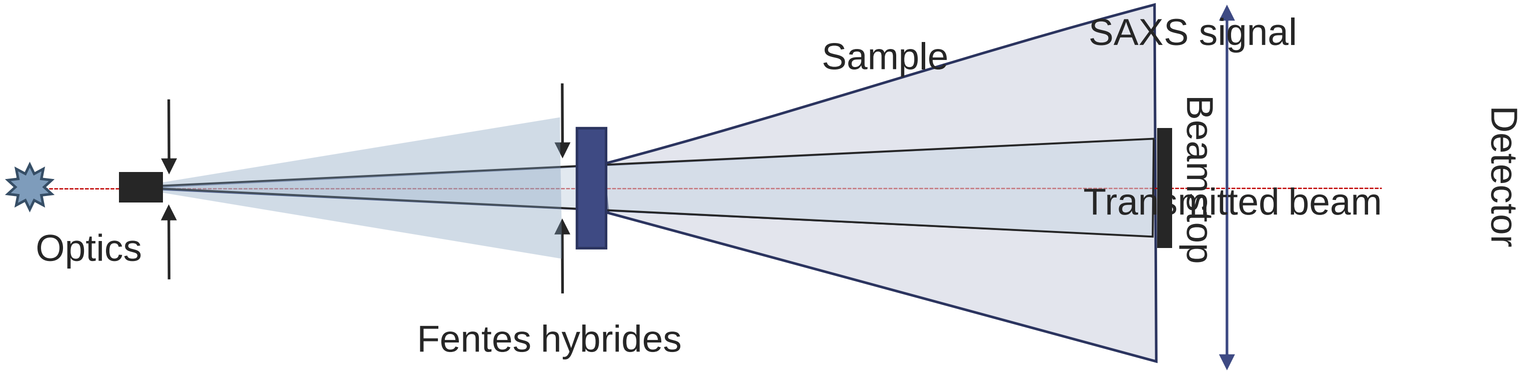

- Smaller beam on the sample
- Higher resolution
- Higher qmin
- More flux

Increasing by x5 the flux on the sample

Sur le Xeuss

S1

S2

Pinholes: fix
Slits : adjustable

2008

research papers

Journal of
Applied
Crystallography

ISSN 0021-8898Received 6 June 2008
Accepted 26 September 2008

Scatterless hybrid metal–single-crystal slit for small-angle X-ray scattering and high-resolution X-ray diffraction

Youli Li,[a]* Roy Beck,[b] Tuo Huang,[c] Myung Chul Choi[b] and Mo

[a]Materials Research Laboratory, University of California at Santa Barbara, Santa B
USA, [b]Materials and Physics Departments, University of California at Santa Barb
CA 93106, USA, and [c]Grinnell College, Grinnell, IA 50112-1690, USA. Corres
youli@mrl.ucsb.edu

A simple hybrid design has been developed to produce practicall
aperture slits for small-angle X-ray scattering and high-resol
diffraction. The hybrid slit consists of a rectangular single-cryst

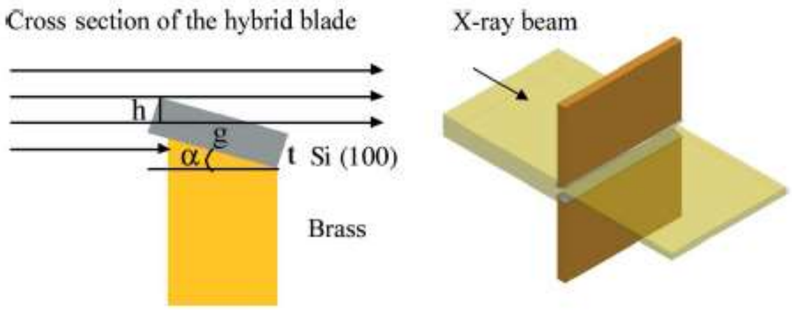

(*a*)

Technical data Sheet

Accessories for SAXS

Hybrid Scatterless Slits

Xenocs

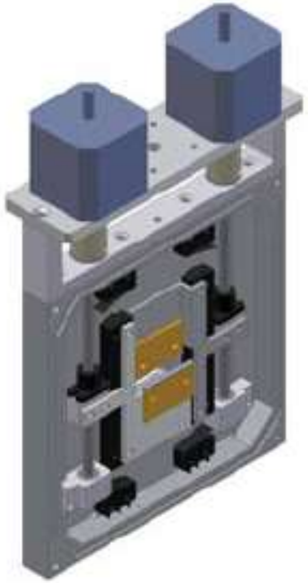

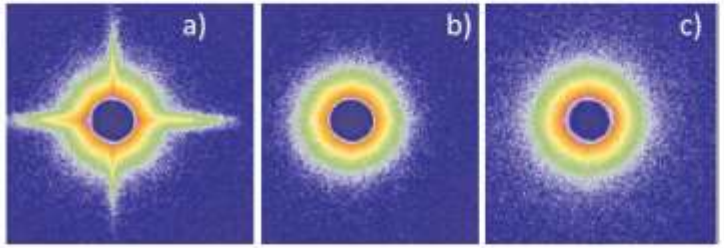

Fig. 3: Images of empty SAXS camera of the D2AM beamline at ESRF, France, collected on a 1.67m SAXS camera and 3mm beamstop, energy set to 17.48keV.

(a) Standard collimation, flux maximized to 3.4e10 ph/s @17.48keV on sample

(b) Same collimation, last anti scatter slits replaced by Xenocs' scatterless slits, same flux

(c) Collimation scheme simplified including Xenocs' scatterless slits allows to increase the flux up to 9.6e10ph/s with same beam focus on detector.

2010-2011 : improved version of the scatterless « collimator »

(12) DEMANDE INTERNATIONALE PUBLIÉE EN VERTU DU TRAITÉ DE COOPÉRATION EN MATIÈRE DE BREVETS (PCT)

(19) Organisation Mondiale de la Propriété Intellectuelle
Bureau international

(43) Date de la publication internationale
3 novembre 2011 (03.11.2011)

PCT

(10) Numéro de publication internationale
WO 2011/135510 A1

(51) Classification internationale des brevets : *G21K 1/02* (2006.01) *G21K 1/06* (2006.01)

(21) Numéro de la demande internationale : PCT/IB2011/051805

(22) Date de dépôt international : 26 avril 2011 (26.04.2011)

(25) Langue de dépôt : français

(26) Langue de publication : français

(30) Données relatives à la priorité : 1001774 26 avril 2010 (26.04.2010) FR

(71) Déposant *(pour tous les États désignés sauf US)* : COMMISSARIAT A L'ENERGIE ATOMIQUE ET AUX ENERGIES ALTERNATIVES [FR/FR]; 25 rue Leblanc, Bâtiment "Le Ponant D", F-75015 Paris (FR).

(72) Inventeurs; et
(75) Inventeurs/Déposants *(pour US seulement)* : TACHE, Olivier [FR/FR]; 43 rue Louise Bruneau, F-91120 Palaiseau (FR). SPALLA, Olivier [FR/FR]; 9 avenue Secrétan, F-75019 Paris (FR).

(74) Mandataires : CABINET ORES et al; 36 rue de St Pétersbourg, F-75008 Paris (FR).

(81) États désignés *(sauf indication contraire, pour tout titre de protection nationale disponible)* : AE, AG, AL, AM, AO, AT, AU, AZ, BA, BB, BG, BH, BR, BW, BY, BZ, CA, CH, CL, CN, CO, CR, CU, CZ, DE, DK, DM, DO, DZ, EC, EE, EG, ES, FI, GB, GD, GE, GH, GM, GT, HN, HR, HU, ID, IL, IN, IS, JP, KE, KG, KM, KN, KP, KR, KZ, LA, LC, LK, LR, LS, LT, LU, LY, MA, MD, ME, MG, MK, MN, MW, MX, MY, MZ, NA, NG, NI, NO, NZ, OM, PE, PG, PH, PL, PT, RO, RS, RU, SC, SD, SE, SG, SK, SL, SM, ST, SV, SY, TH, TJ, TM, TN, TR, TT, TZ, UA, UG, US, UZ, VC, VN, ZA, ZM, ZW.

(84) États désignés *(sauf indication contraire, pour tout titre de protection régionale disponible)* : ARIPO (BW, GH, GM, KE, LR, LS, MW, MZ, NA, SD, SL, SZ, TZ, UG, ZM, ZW), eurasien (AM, AZ, BY, KG, KZ, MD, RU, TJ, TM), européen (AL, AT, BE, BG, CH, CY, CZ, DE, DK, EE, ES, FI, FR, GB, GR, HR, HU, IE, IS, IT, LT, LU, LV, MC, MK, MT, NL, NO, PL, PT, RO, RS, SE, SI, SK, SM, TR), OAPI (BF, BJ, CF, CG, CI, CM, GA, GN, GQ, GW, ML, MR, NE, SN, TD, TG).

Publiée :
— *avec rapport de recherche internationale (Art. 21(3))*

(54) Title : OPTICAL DEVICE FOR ANALYZING A SPECIMEN BY THE SCATTERING OF AN X-RAY BEAM AND ASSOCIATED COLLIMATION DEVICE AND COLLIMATOR.

(54) Titre : DISPOSITIF OPTIQUE POUR ANALYSER UN ECHANTILLON PAR DIFFUSION D'UN FAISCEAU DE RAYONS X, DISPOSITIF DE COLLIMATION ET COLLIMATEUR ASSOCIES.

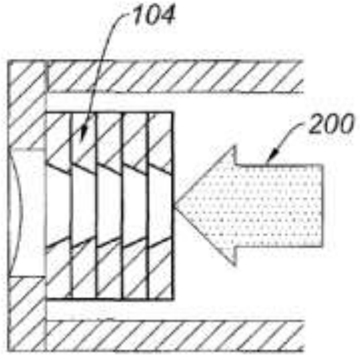

(57) Abstract : The invention relates to a collimation device for an X-ray beam, to an optical device for analysing a specimen (105) by the scattering of an X-ray beam, and a collimator for an X-ray beam. The collimation device comprises an enclosure (110) intended to be under a vacuum or a controlled atmosphere, the enclosure (110) having an inlet (120) and an outlet (121) for the beam and at least one plate (104) made of a material having a diffracting periodic structure, said plate (104) having two main faces (104a, 104b) and at least one flared aperture (104c) between said faces.

(57) Abrégé : L'invention concerne un dispositif de collimation pour un faisceau de rayons X, un dispositif optique pour analyser un échantillon (105) par diffusion d'un faisceau de rayons X et un collimateur pour un faisceau de rayons X. Le dispositif de collimation comprend une enceinte (110) destinée à être mise sous vide ou sous atmosphère contrôlée, l'enceinte (110) comportant une entrée (120) et une

13551 A1

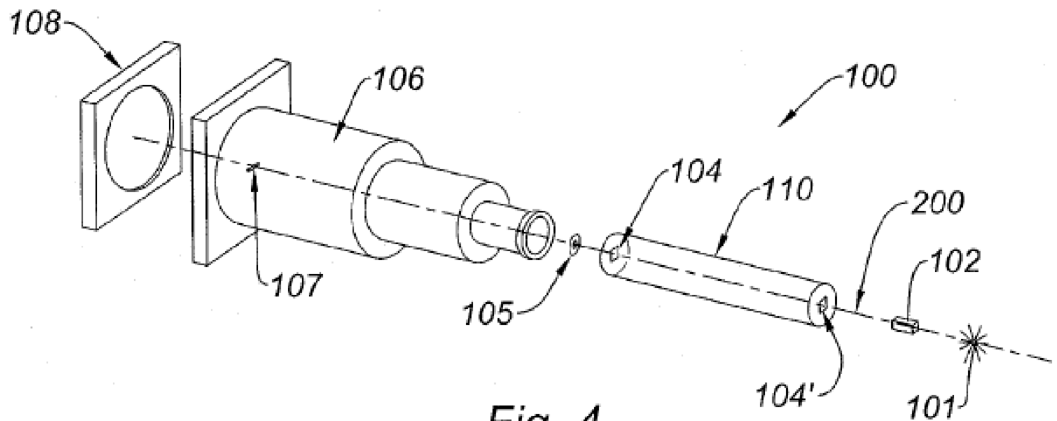

Fig. 4

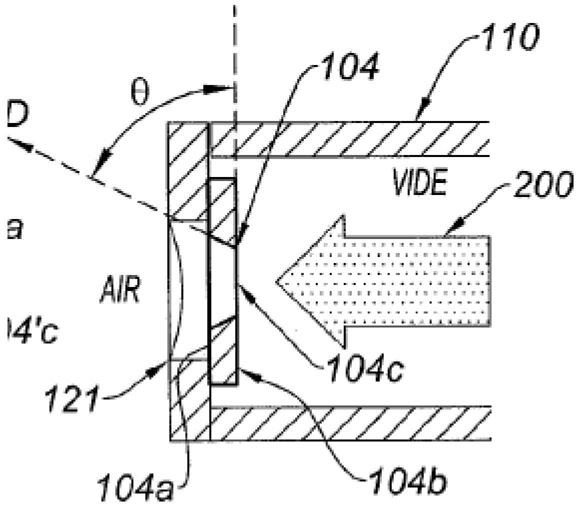

Fig. 6

2012 Xenocs patent transfer

xenocs
Exploring the very small

Comparative tests

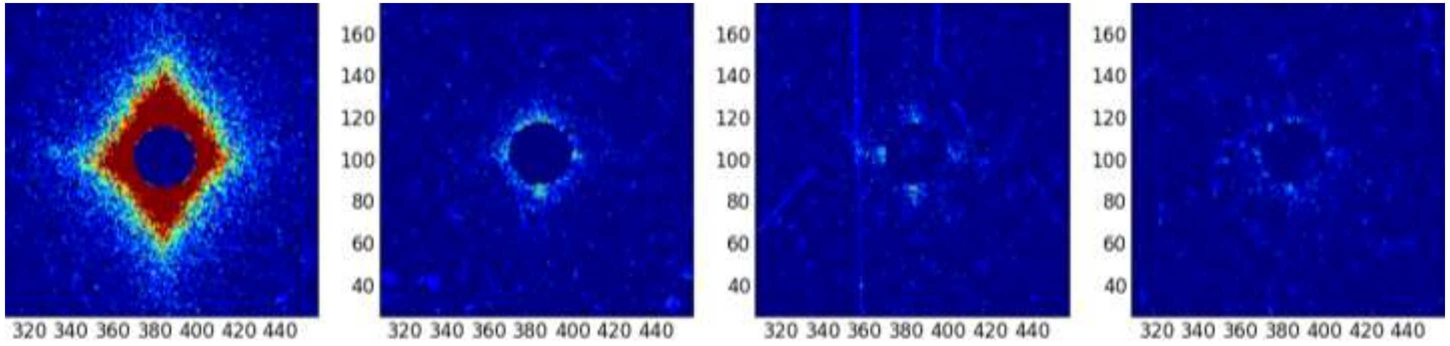

Old system | V1 | V2 | V3

Parasitic Diffusion

Scattering signal of Air
Scattering signal of windows

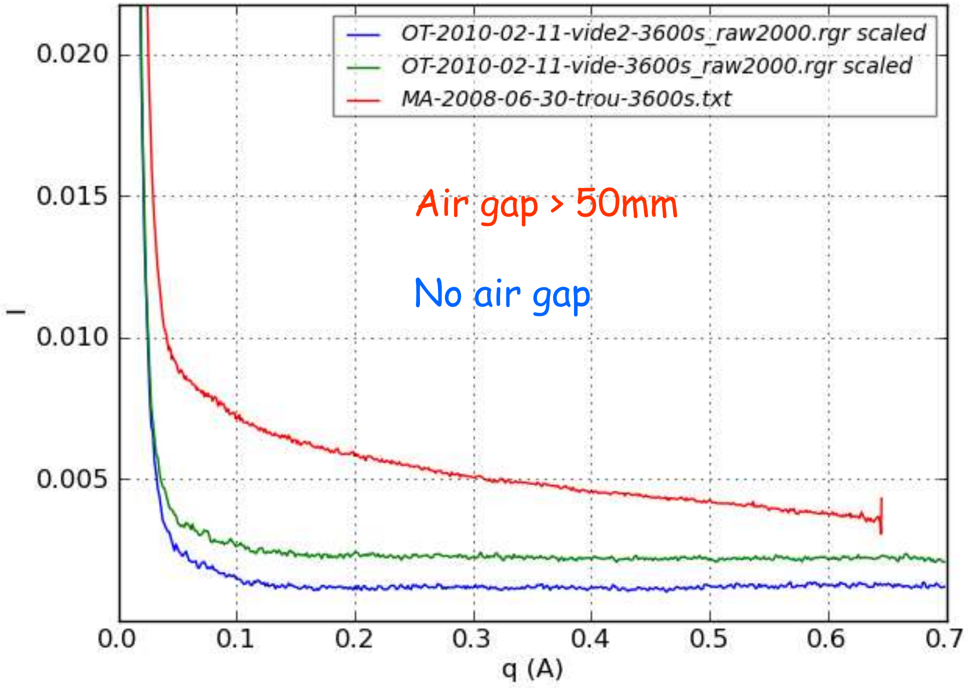

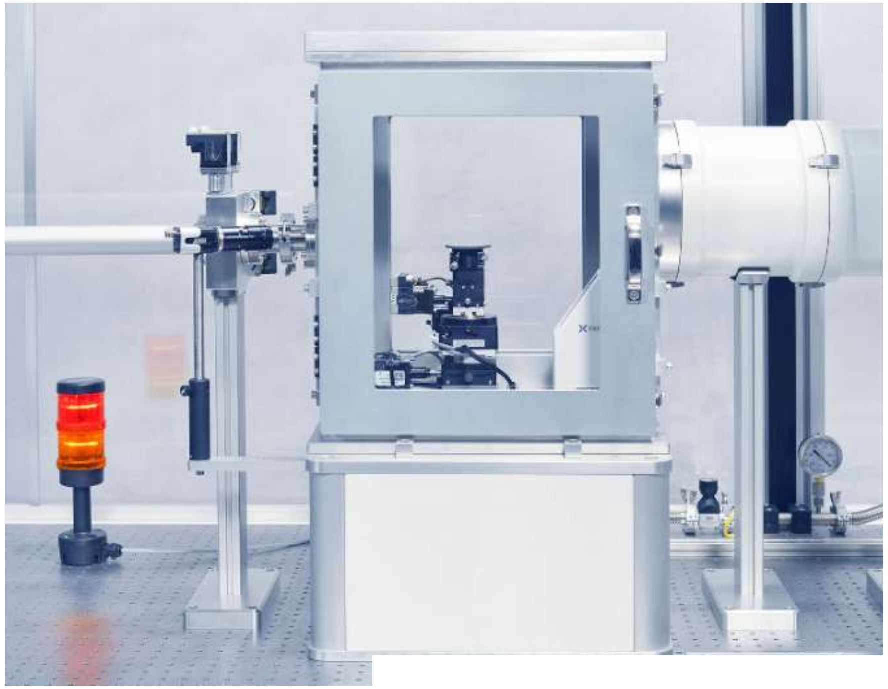

SAXS windows on XEUSS 2

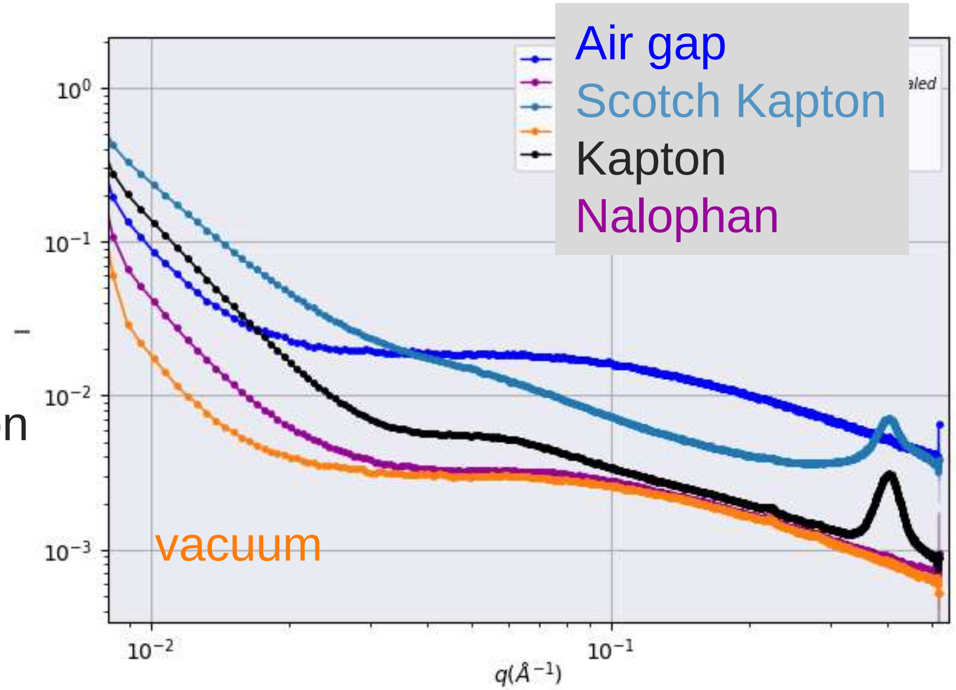

BEAMSTOP

Stop the direct beam

- do not damage the detector
- avoid detector/chamber windows diffraction
- Must be inside the vacuum chamber
- coupled with a photodiode

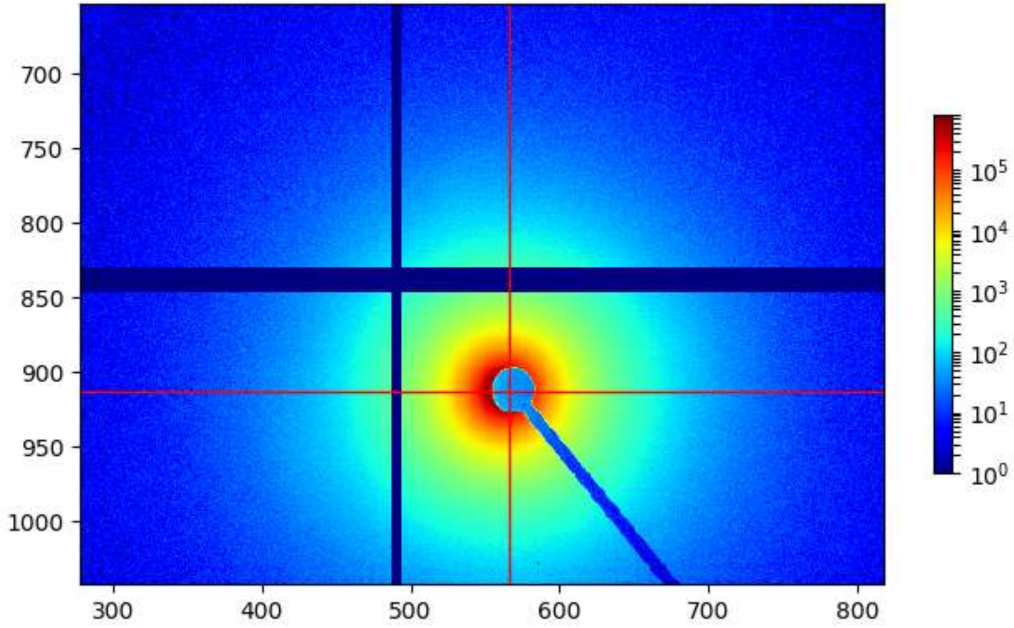

Beamstop less configuration

- ANTON PAAR
- XENOCS

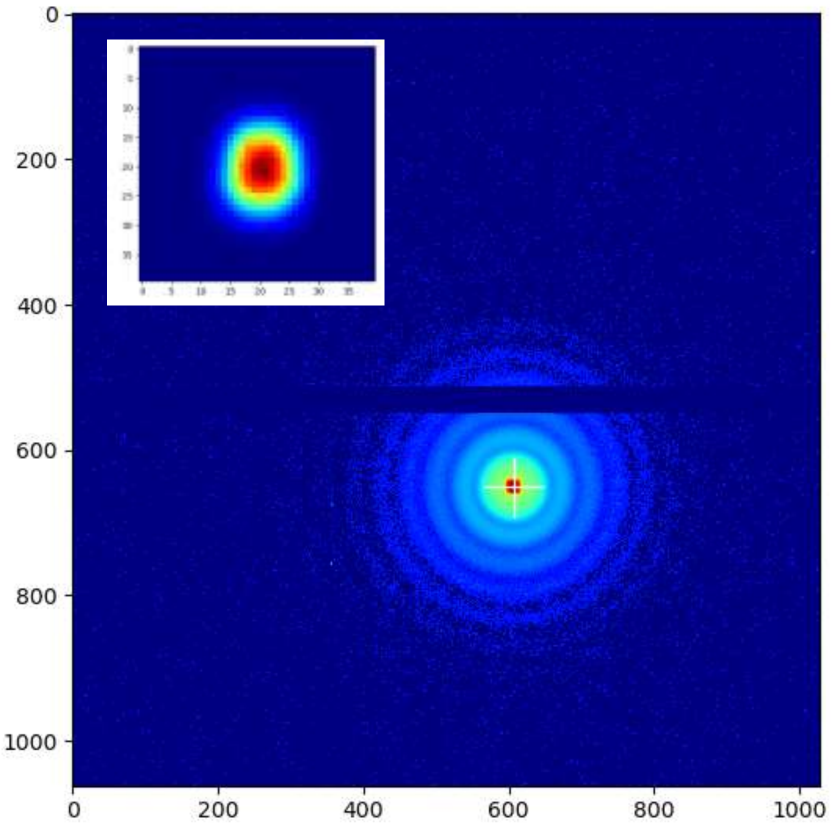

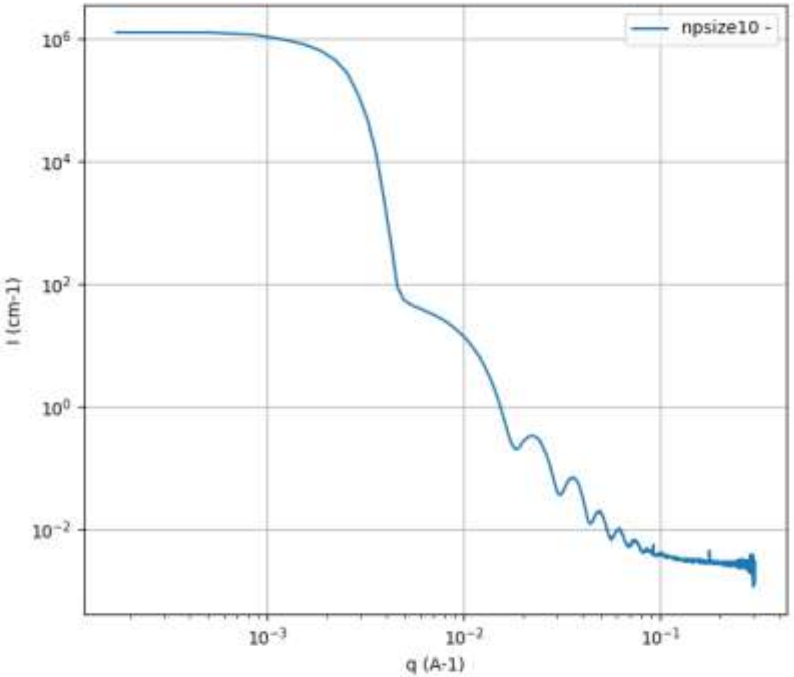

- Need of Eiger detector (frame rate)
- Image data treatment

- **Improve the absolute intensities**

Détection

Instruments de réglage

- Scintillateurs
- Photodiode
- Camera vidéo

Caractéristiques requises pour l'imagerie en SAXS (laboratoire)

- Taille de détection >100 mm
- Sensibilité :
  - Bruit de fond faible
  - Temps de comptage long
- Résolution ? (taille du faisceau 1x1 mm)

Scintillateur

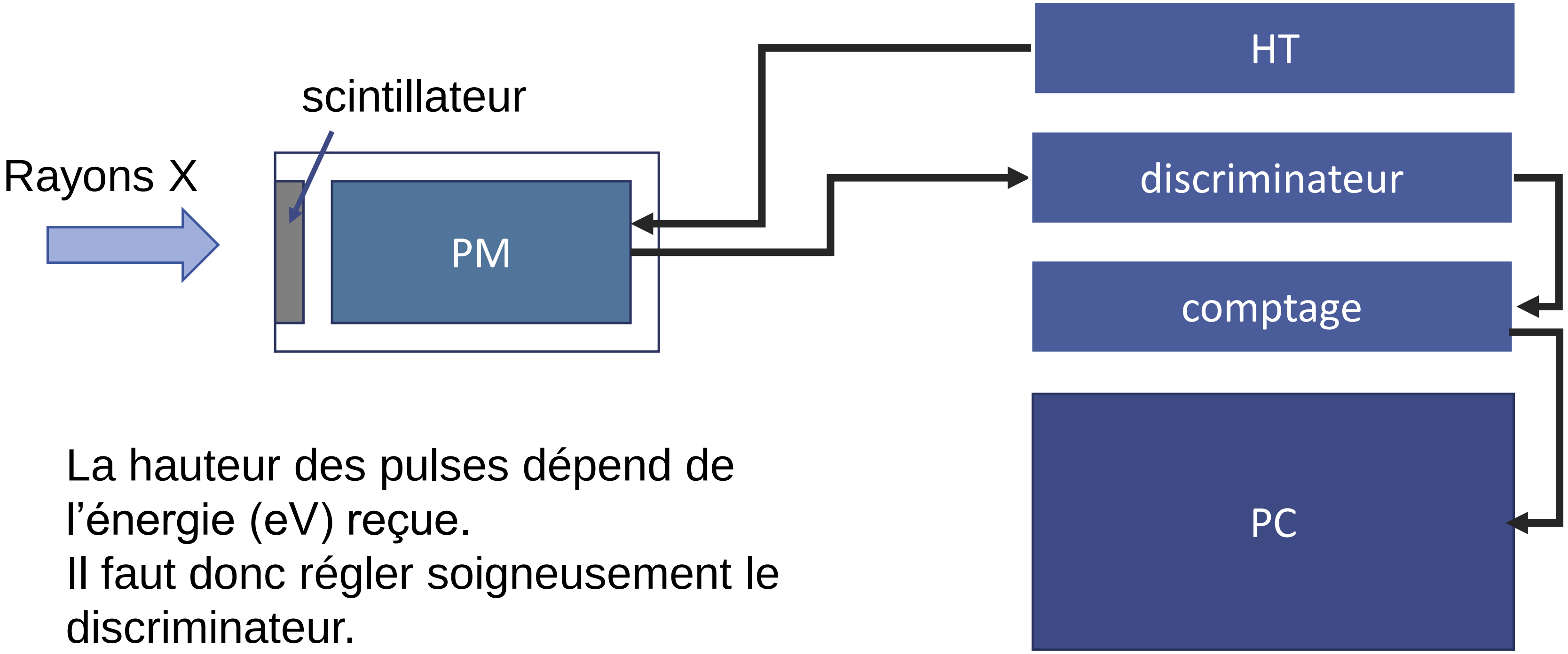

La hauteur des pulses dépend de l'énergie (eV) reçue.
Il faut donc régler soigneusement le discriminateur.

Bruit de fond élevé, Détecteur 1D

Photodiode

Calibrated photodiode
3.4 mm x 1.3 mm
Si Thickness 52 µm

$$i = F_0 * A * \frac{E}{3,65\ eV} * q$$

- F_0, incident flux (ph/s)
- A absorbance of 52µm Si at 8 keV : 55%
- E energy (8keV)
- Q= $1,6 * 10^{-19}$ C
- One signal electron in silicon requires 3.65 eV

1nA → 5.10^6 ph/s

Bruit de fond élevé, Détecteur 1D

Détecteurs 2D : Camera CCD

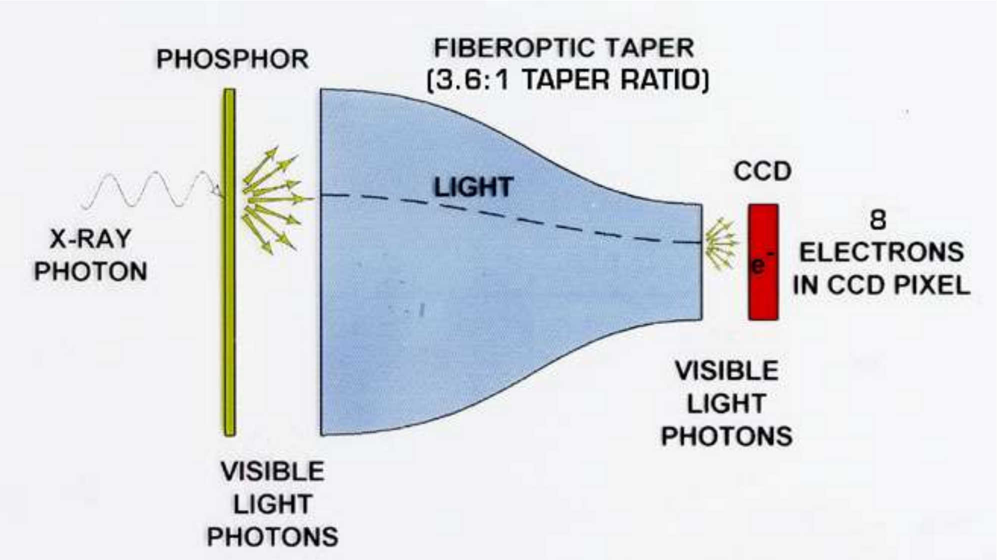

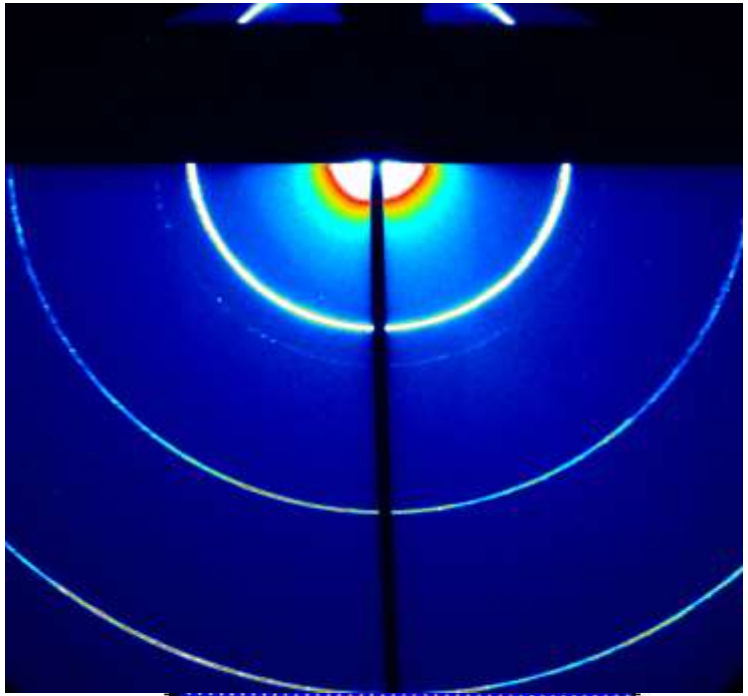

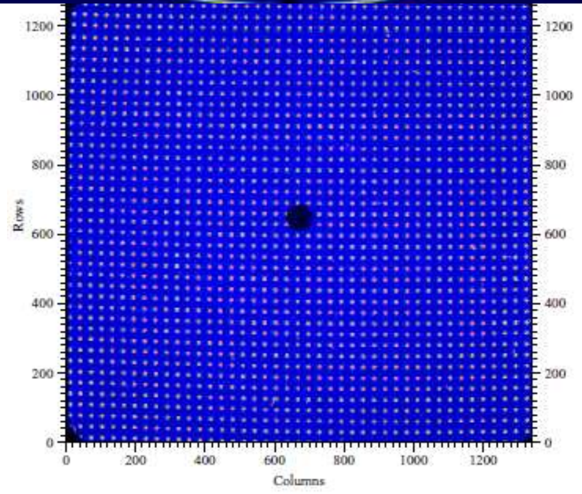

Caractéristiques

+ taille des pixels (10 a 20 µm)
+ vitesse d'acquisition (<5s)

- bruit de lecture + bruit électronique
- Prix / Taille,
- Cosmiques,
- distorsion de l'image (selon capteur)

Détecteur à gaz

Principe de fonctionnement:

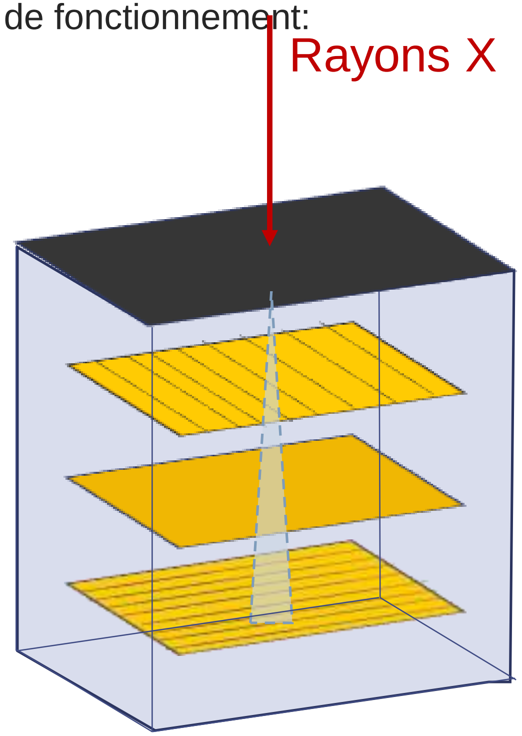

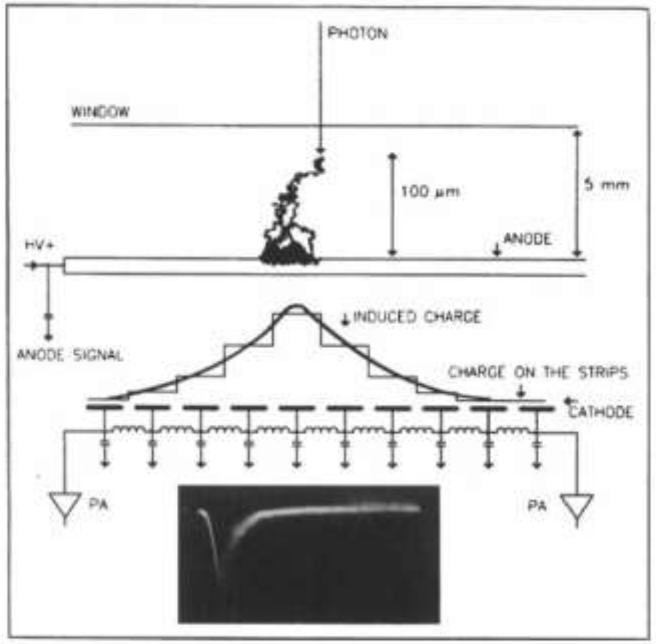

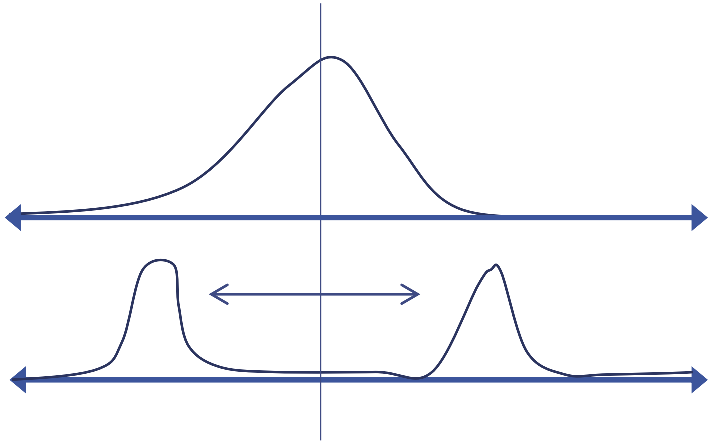

Menhard Kocsis, *"The status of gas-filled detector developments at a third generation synchrotron source (ESRF)"*, Nuclear Instruments and Methods in Physics Research A 471 (2001) 103–108

Petrascu, A. -M. , Koch, M. H. J. and Gabriel, A'*A beginners' guide to gas-filled proportional detectors with delay line readout'*, Journal of Macromolecular Science, Part B, 37: 4, .(1998) 463 — 483

Détecteur à gaz

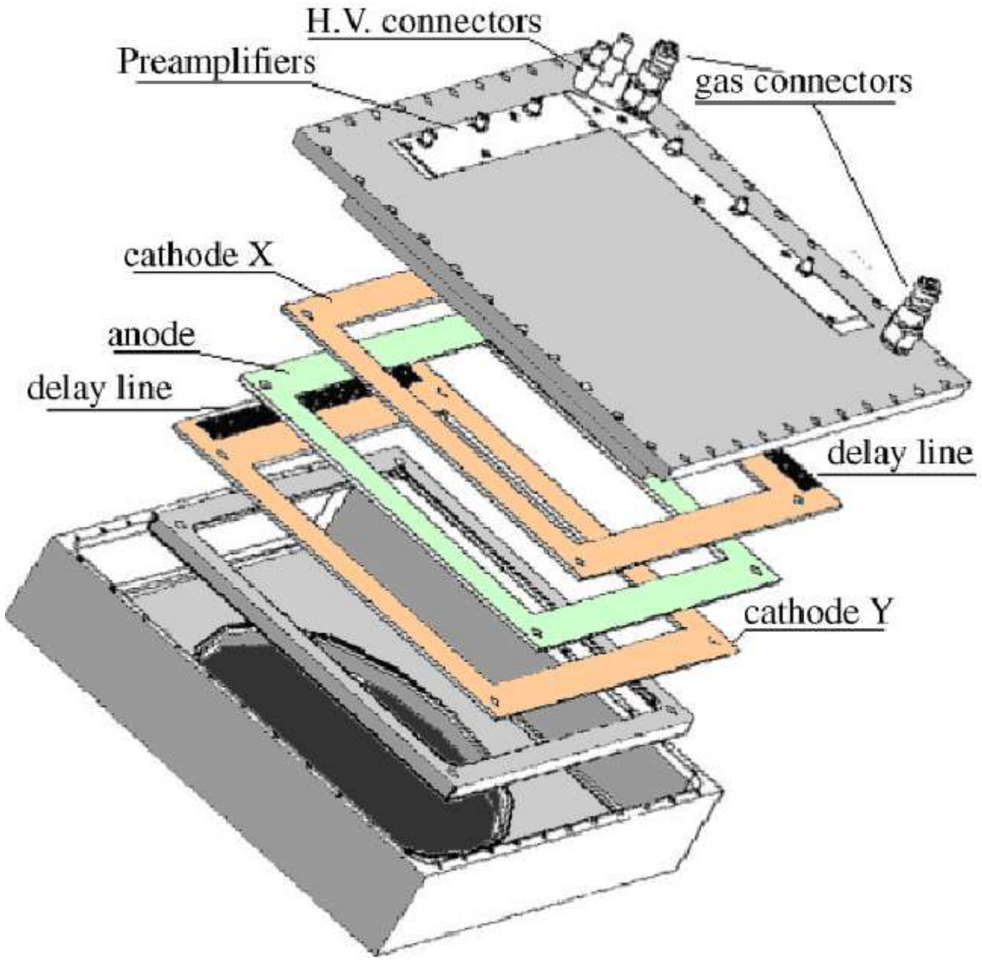

Fig. 1. Exploded view of the delay line based detector.

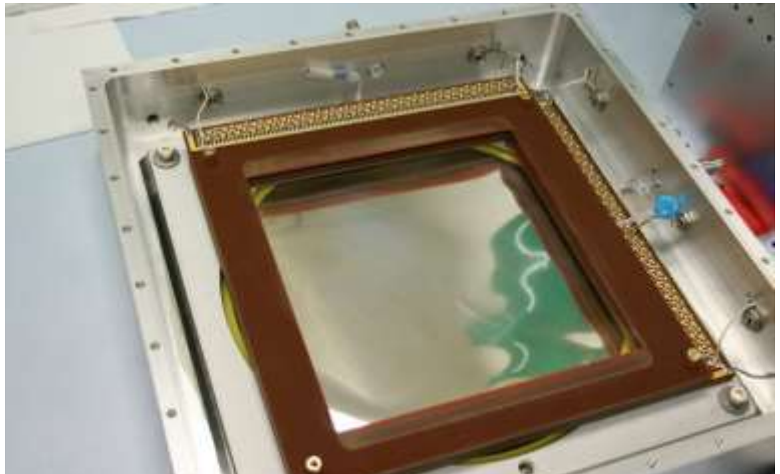

Photo du détecteur « lure » type Gabriel

Plan de fils de la grille d'anode

Caractéristiques :

+ Bruit de fond très bas (typiquement 100 cps/s sur tout le détecteur)
+ grille de 512x512
+ Résolution à 8 keV de 500 µm

+ 4-20 keV
+ lecture en continu
+ Gaz : Ar CO_2 pour 8 keV

- Moins de 10^6 photons/s
- Très fragile
- Distorsion si grille réparée
- réparation

Détecteurs 2D : Image Plate Mar

Principe de fonctionnement

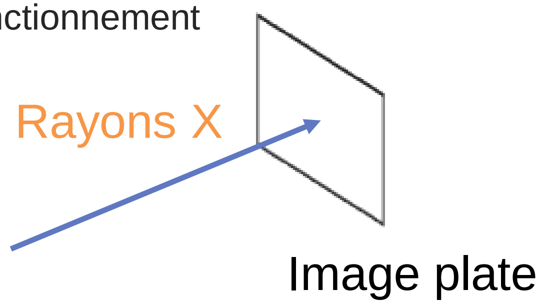

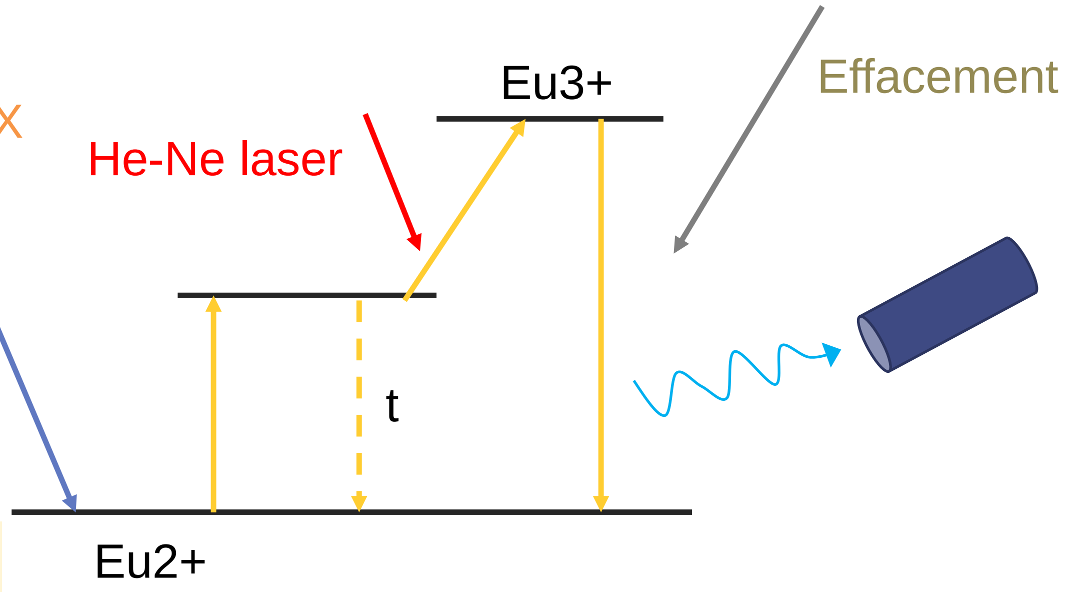

Caractéristiques

+Taille (jusqu'à 345 mm)
+Prix /taille
+Pas de distorsion
+ Efficacité (90%)
+ Temps de lecture (2 min)
+ Lecture automatique

-Bruit de fond
-Encombrement
- Système fermé (pas pour LIONS)

39

Détecteur 2D : Mar

Image plate circulaire avec scanner

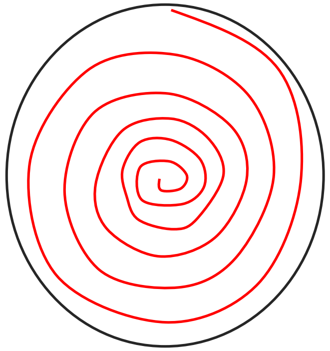

- Effacement automatique

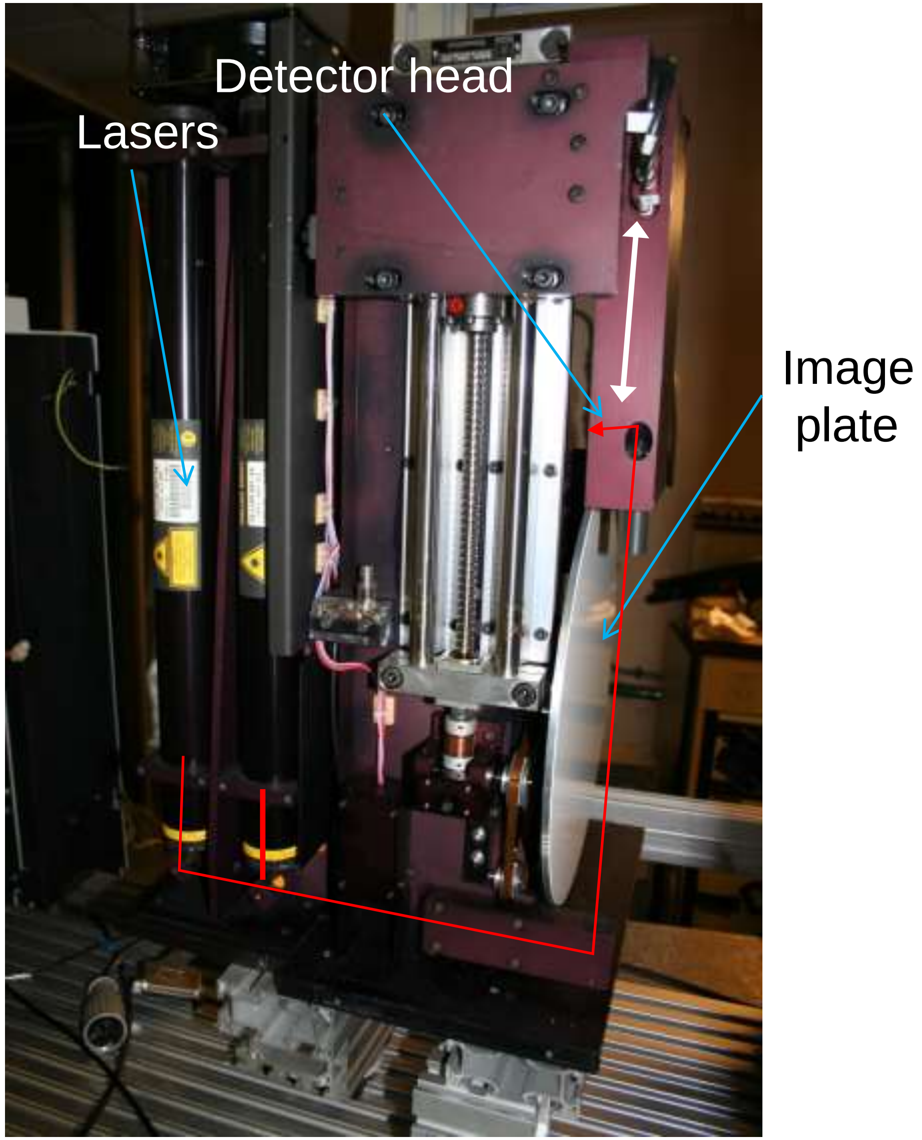

Détecteur 2D : Mar

Pour garder un écartement identique (100µm),
la vitesse de rotation augmente quand le rayon diminue

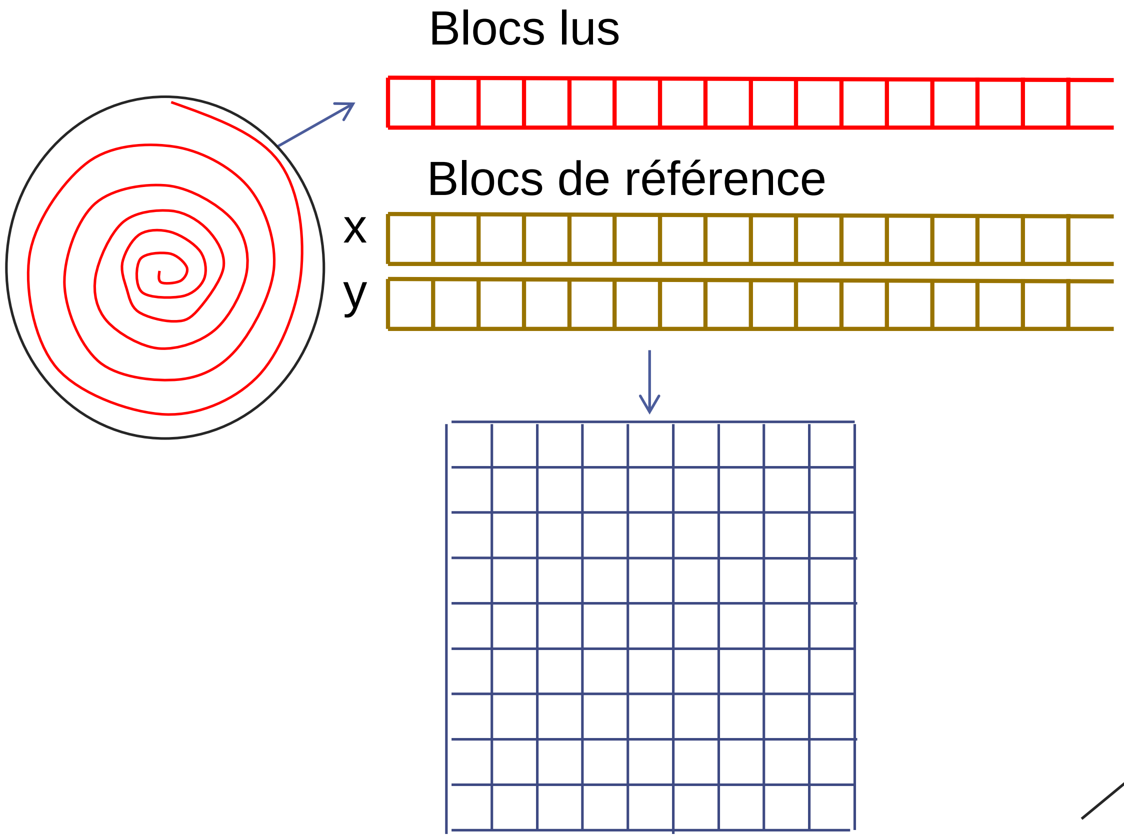

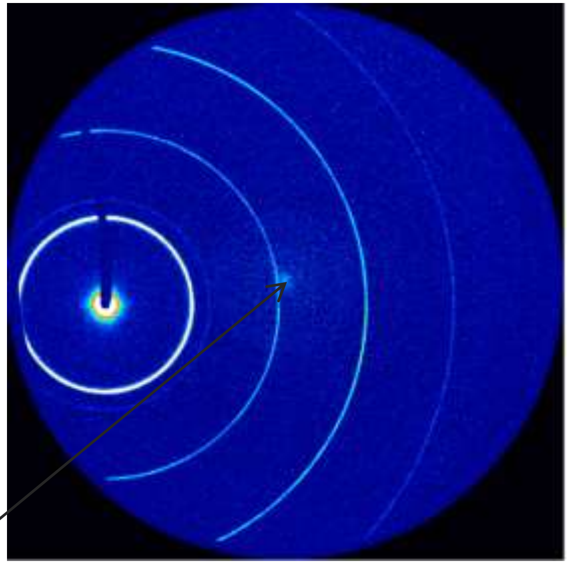

Problème de reconstruction d’image au centre (surestimation de la valeur des pixels)

PILATUS : DETECTEUR hybride A PIXEL

Combinaison technologie
détecteur à gaz et électronique

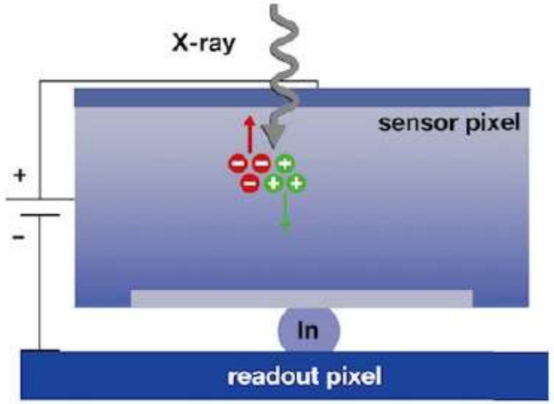

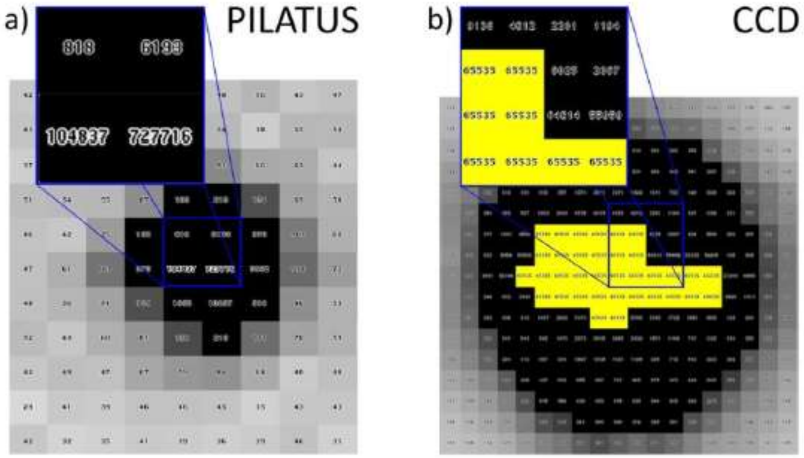

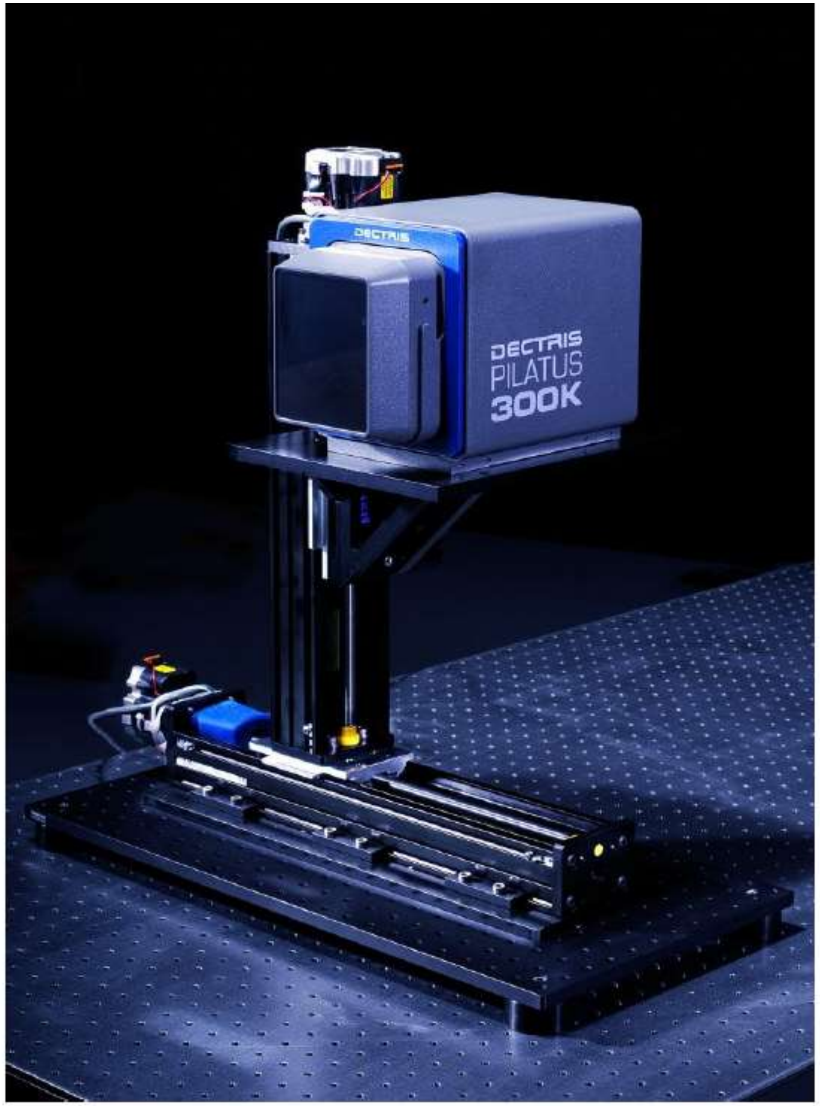

FONCTIONNEMENT DU PILATUS

Maximum count rate [phts/s/pixel] $1 \cdot 10^7$
Counter depth 20 bits (1,048,576 counts)

Number of detector modules	1 x 2	2 x 5
Sensitive area (width x height) [mm^2]	83.8 x 70.0	168.7 x 179.4
Pixel size [µm^2]	172 x 172	172 x 172
Total number of pixels	487 x 407 = 198,209	981 x 1043 = 1,023,183

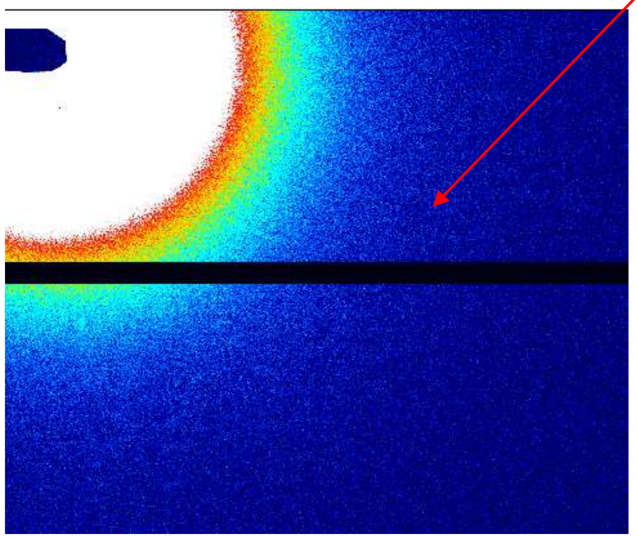

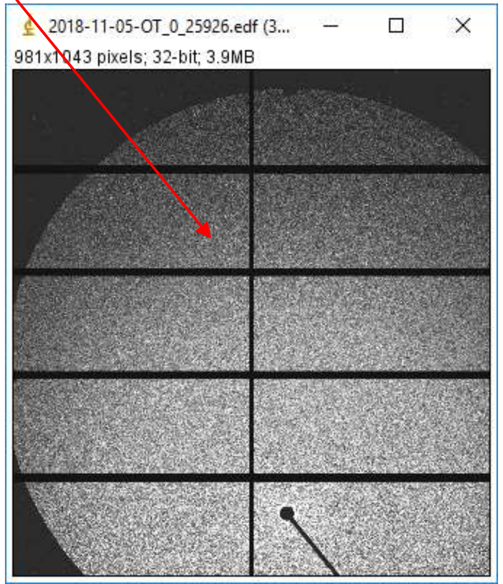

XEUSS 3 DECTRIS EIGER2 1M

- Under vacuum
- Fast read-out (enable beamstop less instrument)
- Lower dark current / background
- Taille détection ?

Superior count-rate performance

DECTRIS HPC detectors are designed to match the high count-rate requirements of synchrotron sources, but on the other hand, even the most advanced laboratory sources offer lower flux and brightness than a typical synchrotron beamline does. Therefore, EIGER2 R detectors far exceed the count-rate requirements of any laboratory set-up and experiment. At the same time, EIGER2 R overcomes the saturation issues and limited dynamic range that are typical of integrating detectors, even modern ones. Thanks to its superior count-rate performance, EIGER2 R is the best match for state-of-the-art laboratory sources. It provides high accuracy for strong intensities, without saturation issues, and even allows for measurement of a direct beam.

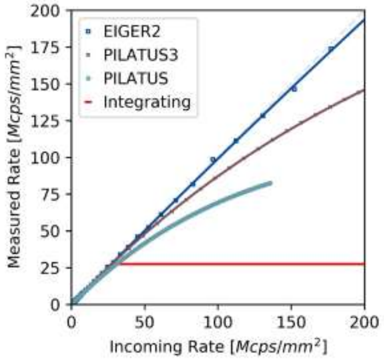

Highest dynamic range

EIGER2 R's zero detector background, superior count rates, and simultaneous read/write provide the highest dynamic range. Determine the highest and lowest intensities accurately and in a single image, whether you are measuring strong and weak reflections or diffuse scattering, or facing a challenging SAXS/WAXS measurement.

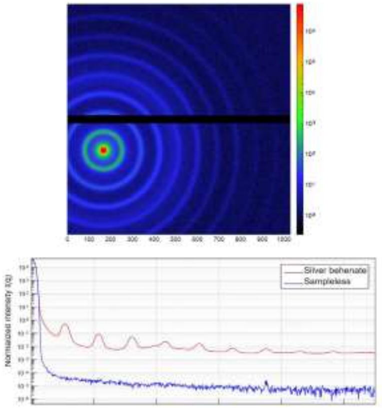

WAXS signal of Silver behenate (AgBH). Top: Raw data acquired with an EIGER2 R 1M in a Xeuss3.0 SAXS/WAXS instrument from Xenocs. Bottom: This dual plot of AgBH's signal and a negative control shows that the dynamic range of EIGER2 R detectors easily covers the more than ten orders of magnitude that are needed for weakly scattering samples.

Background suppression

The dual-energy discrimination of EIGER2 R enables suppression of both low- and high-energy background. A single energy-discriminating threshold, as implemented in any HPC detector, allows for the suppression of low-energy background. This is a tremendous advantage when dealing with X-ray fluorescence from the sample or low-energy contamination in the spectrum of the X-ray beam. However, with a second energy-discriminating threshold, as implemented in EIGER2, it is possible to suppress high-energy background as well. Cosmic radiation is a source of high-energy background that compromises data quality when measuring very weak signals with long exposure times. EIGER2 R achieves a fivefold reduction of high-energy background from cosmic radiation, which ensures better data quality. If there is high-energy contamination of the X-ray beam, such as higher-order harmonics, dual-energy discrimination becomes even more critical. Thanks to their lack of detector background and their extensive capabilities for suppression of experimental background with dual-energy discrimination, EIGER2 R detectors are your best choice for measuring weak intensities with high accuracy.

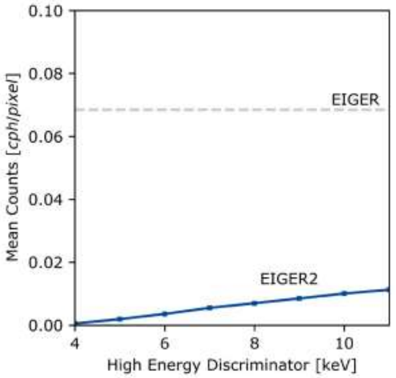

Background counts per pixel in 1 hour dark images. Grey dotted line: Dark counts for EIGER with a single energy discriminator set at 4 keV. Blue solid line: Dark counts for EIGER2 R with a low-energy discriminator at 4 keV as a function of a high-energy discriminator setting.

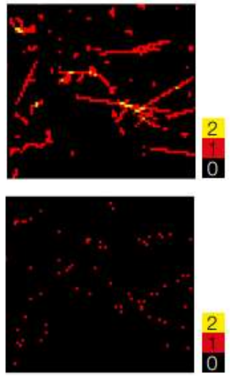

Identical regions obtained through a 1 hour dark exposure of an EIGER2 R detector. Top: Counts obtained with a low-energy discriminator at 4 keV. Bottom: The difference between the counts with a high-energy discriminator at 10 keV and the counts with a low-energy discriminator at 4 keV.

Comparaison Pilatus 1M Eiger 1M

	PILATUS R 1M	PILATUS 300K	EIGER2 1M
Active area (W x H) (mm2)	168.7 x 179.4	83.8 x 70.0	77.1 × 79.7
Pixel size (W x H) [µm2)	172 x 172	172 x 172	75 × 75
Maximum count rate [cps/mm2]	1.00E+08	1.00E+08	9.80E+08

Gain en gamme de q

Chemsaxs	120cm	0.01	à 0.35 A-1
Xeuss2	120 cm	0.01	à 0.5 A-1
Xeuss3	90 cm		

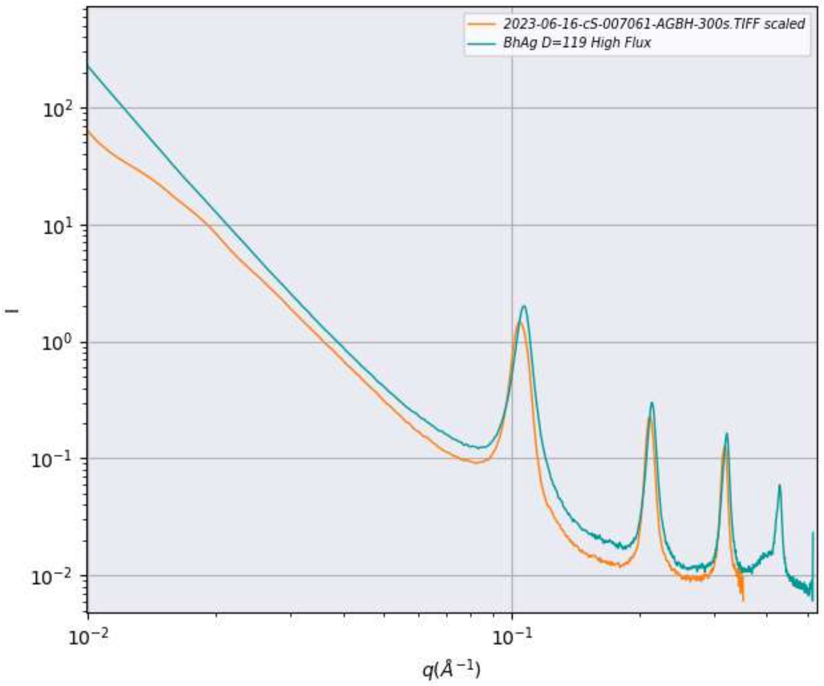

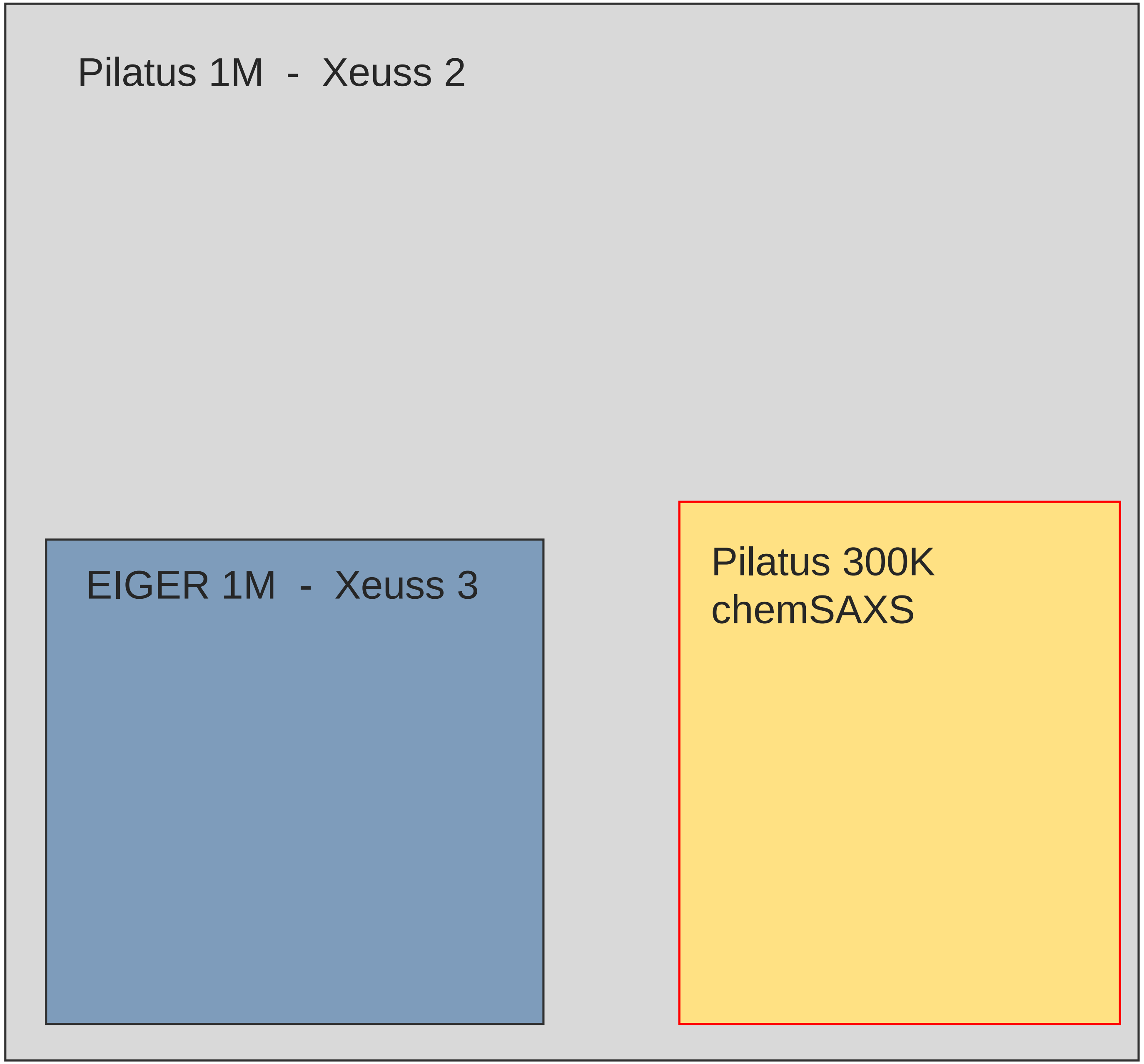

Dark measurements

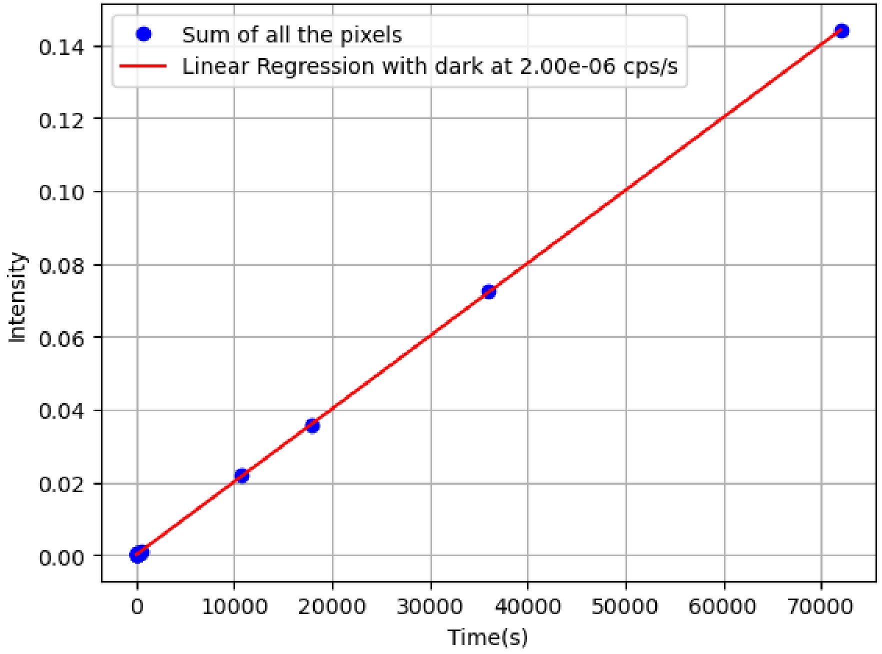

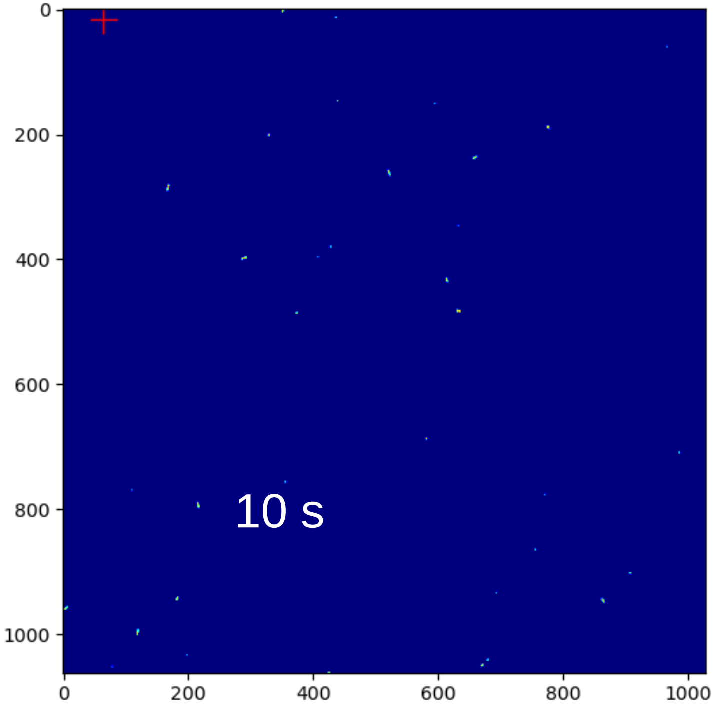

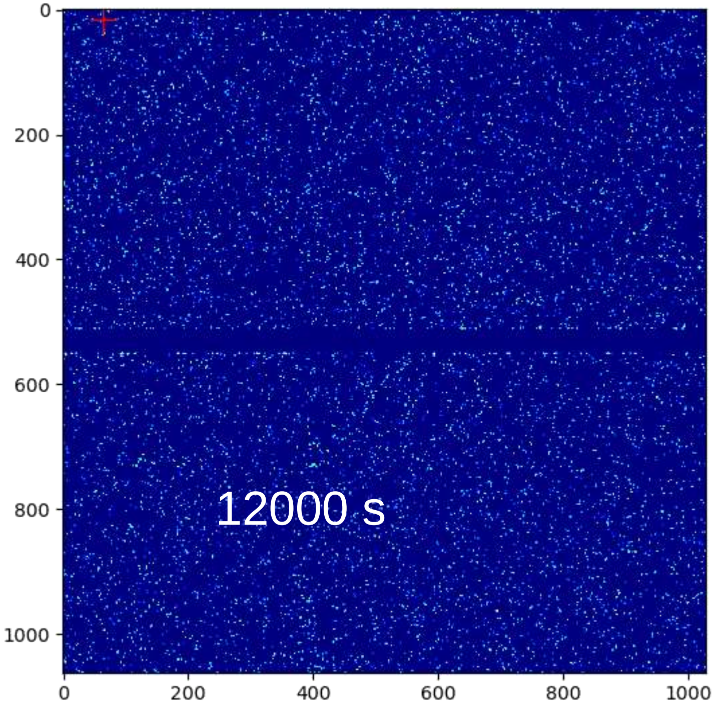

Xeuss 3 / Eiger 1M

DATA TREATMENT

SAXS Data Correction Sequence

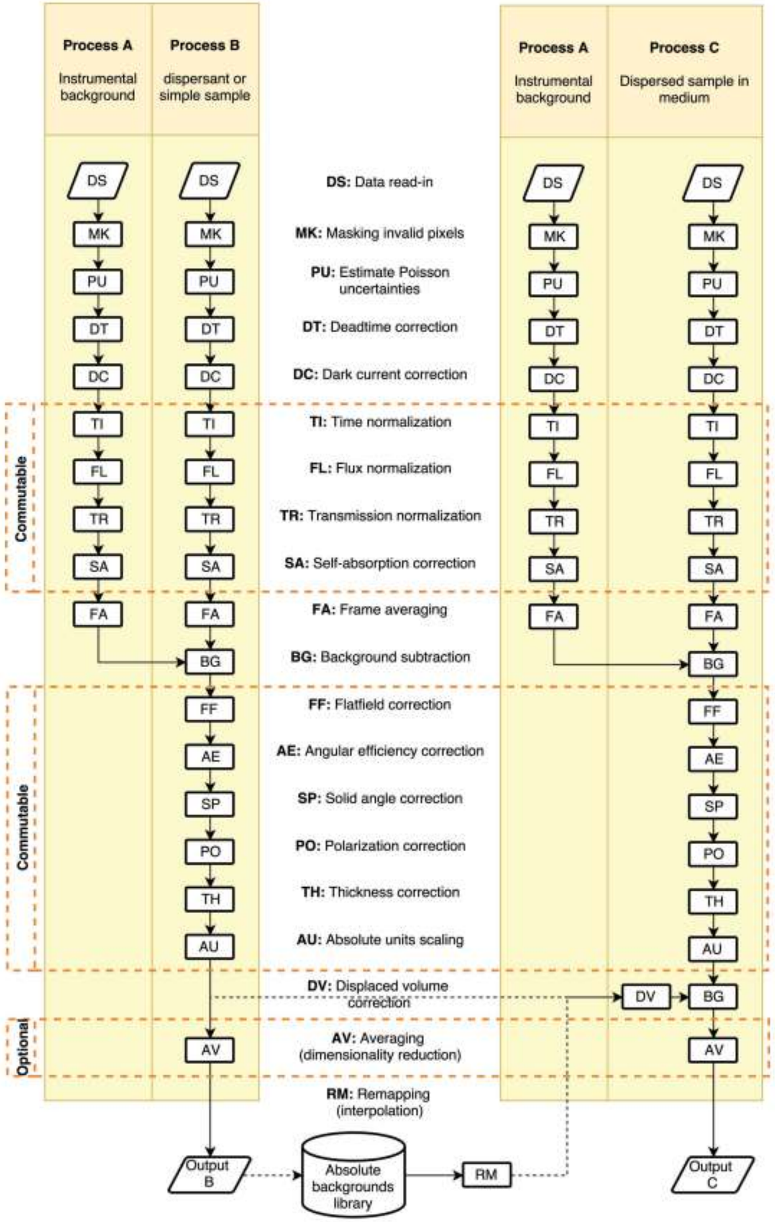

JOURNAL OF APPLIED CRYSTALLOGRAPHY

ISSN 1600-5767

The modular small-angle X-ray scattering data correction sequence

B. R. Pauw,[a*] A. J. Smith,[b] T. Snow,[b] N. J. Terrill[b] and A. F. Thünemann[a]

[a]Bundesanstalt für Materialforschung und -prüfung (BAM), 12205 Berlin, Germany, and [b]Diamond Light Source Ltd, Diamond House, Harwell Science and Innovation Campus, Didcot, Oxfordshire OX11 0DE, UK. *Correspondence e-mail: brian.pauw@bam.de

Received 20 June 2017
Accepted 17 October 2017

Image Data correction

- masking pixels
- Distortion
- 2D radial averaging

1D diagram

- Time
- Flux
- dark

Absolute intensities

- Thickness
- Solvent subtraction

DATA TREATMENT

Image Data Correction

Image Data treatment : 2D radial averaging

- Open the image
- Geometrical correction
- Radial averaging :
- Integration and statistics of all the pixels at the same distance from the beam center

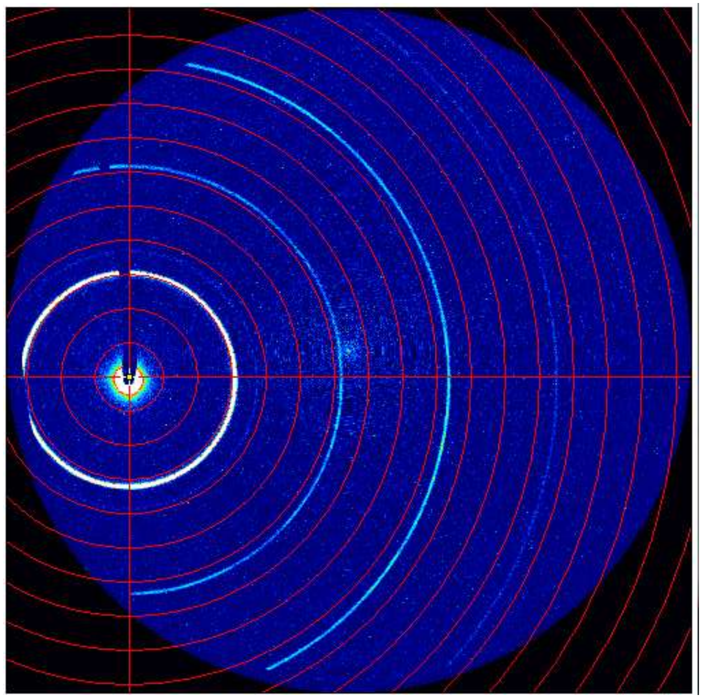

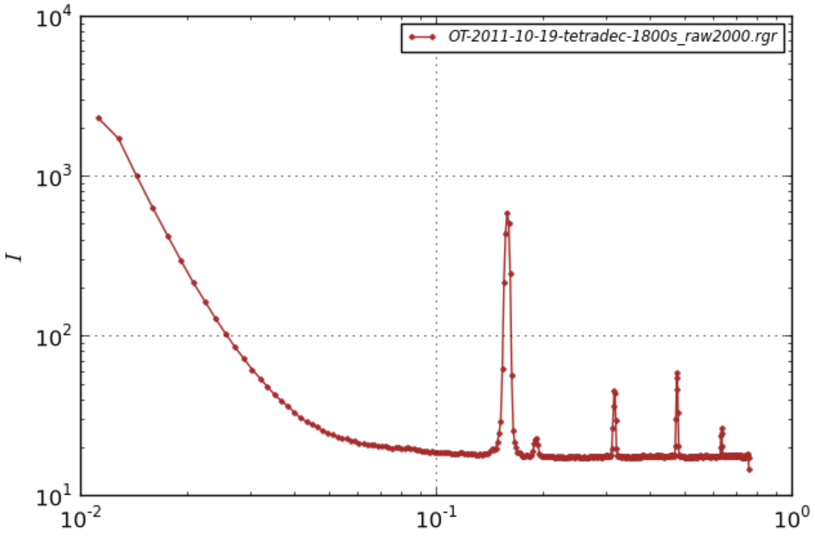

1- define the center and the geometrical parameters of the experiment (center, rotation angles,…)
2- define the masks pixels (beamstop, dead pixels,…)
3- define the Region Of Interest

SAXS Image Data Treatment : geometrical correction

Detector perpendicular to the direct beam

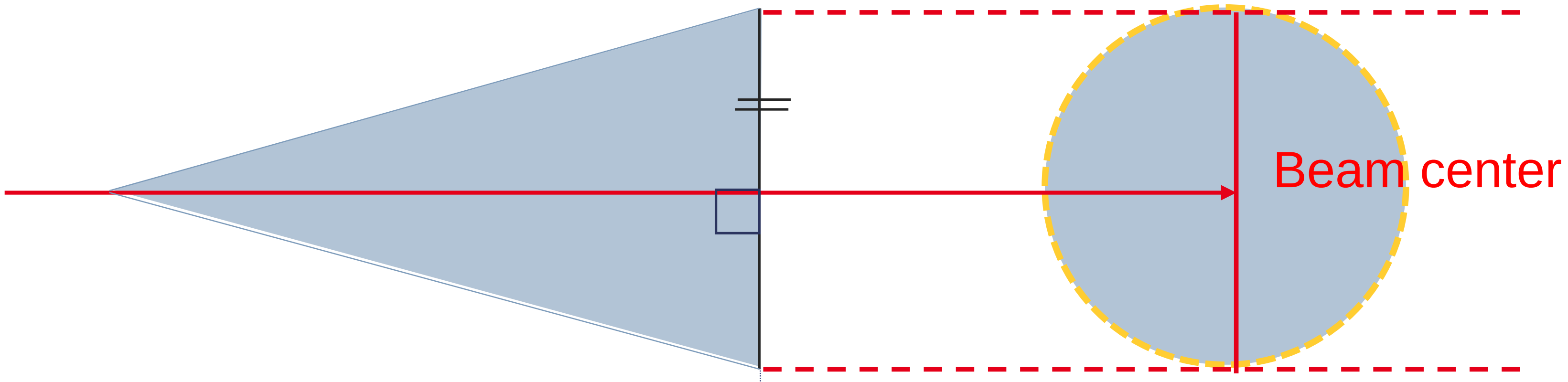

Circle

Detector is tilted

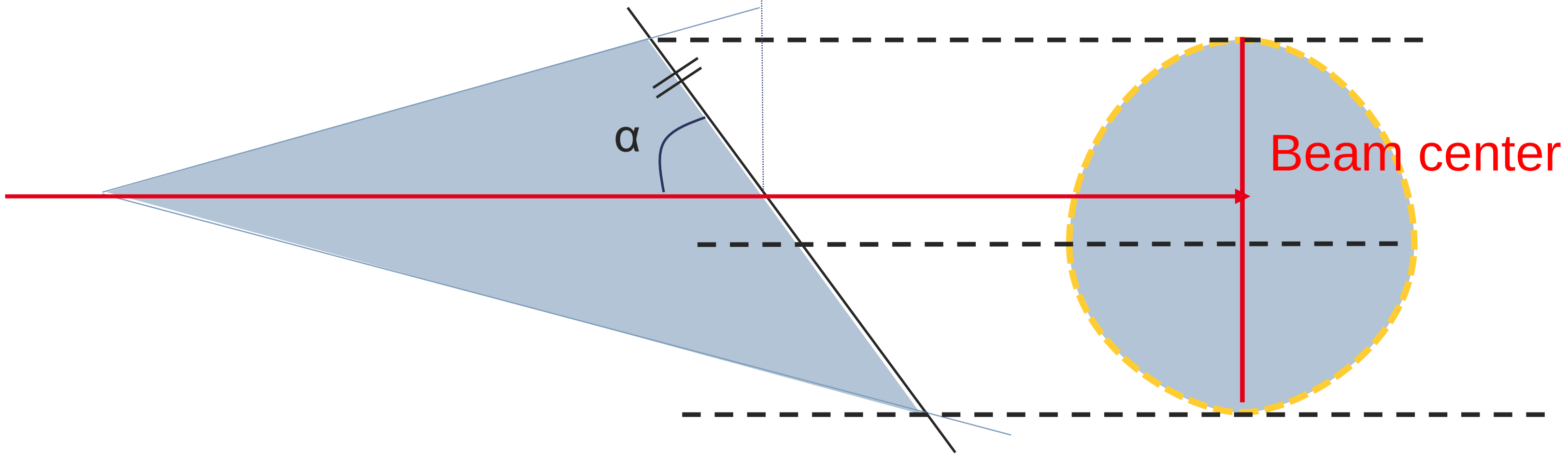

Centers of ellipses are different than the direct beam center

Image Data Treatment : geometrical correction (ImageJ)

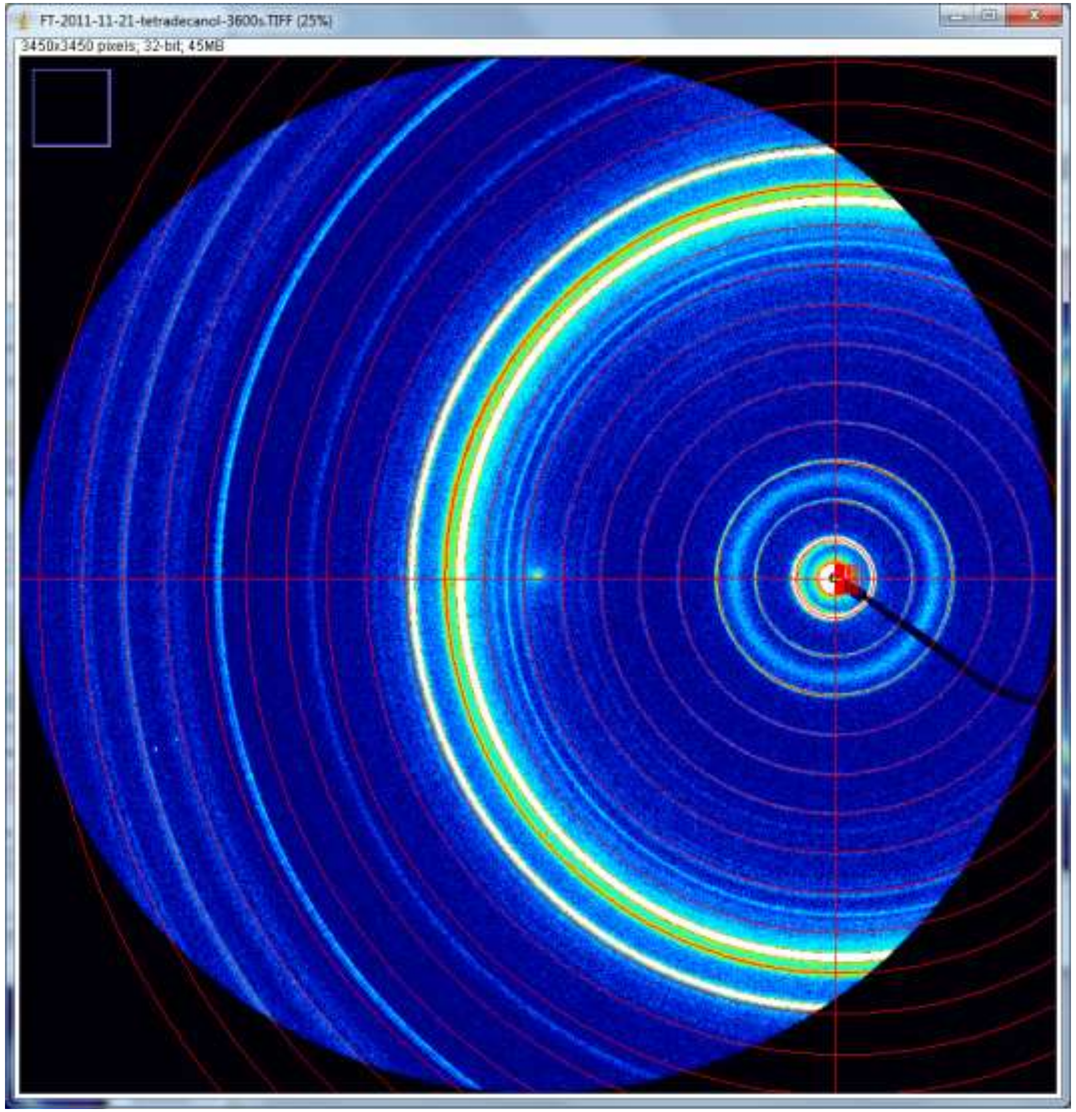

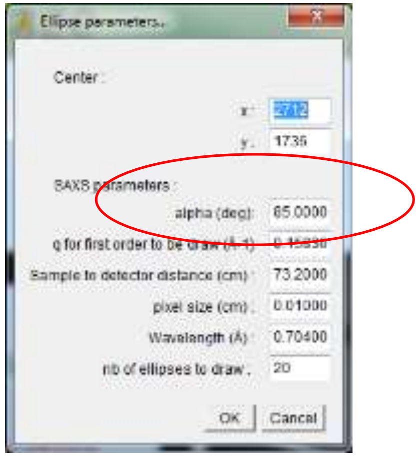

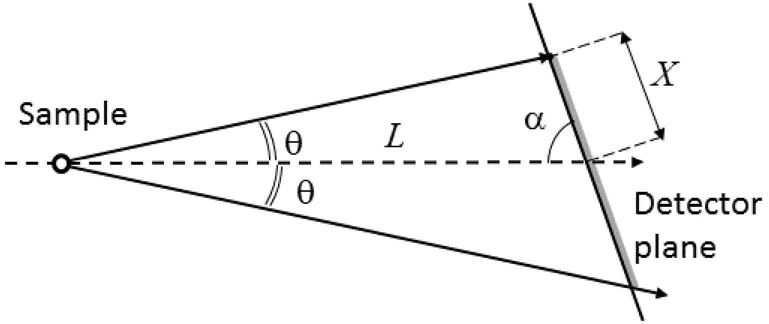

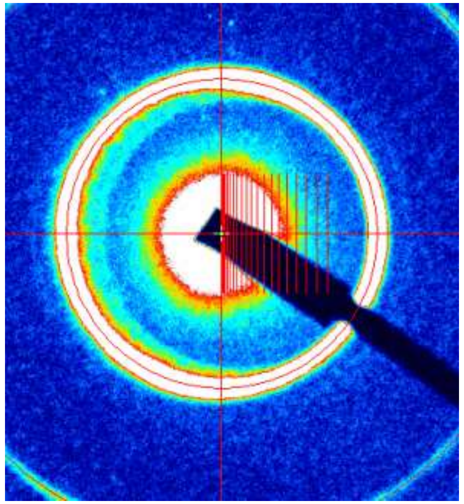

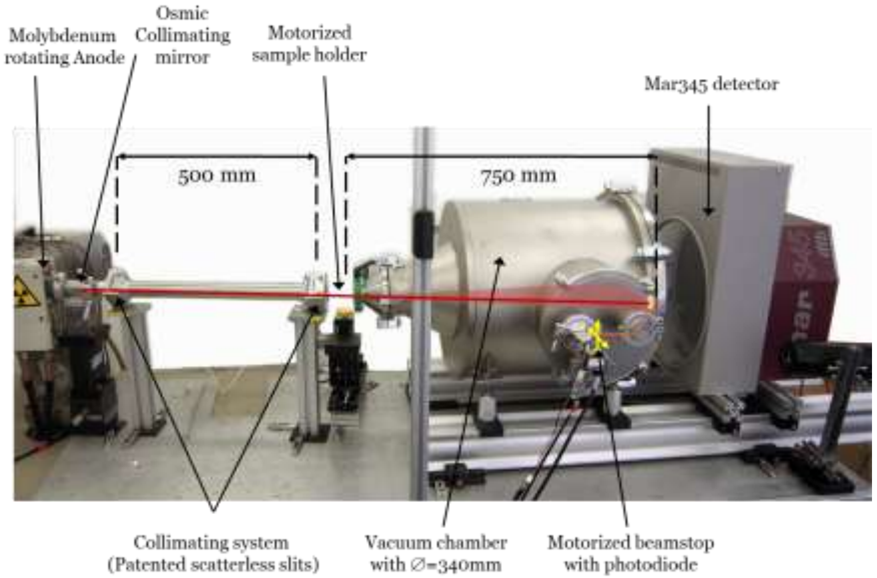

Ag Behenate / MOMAC

Calibrant samples

Ag Behenate

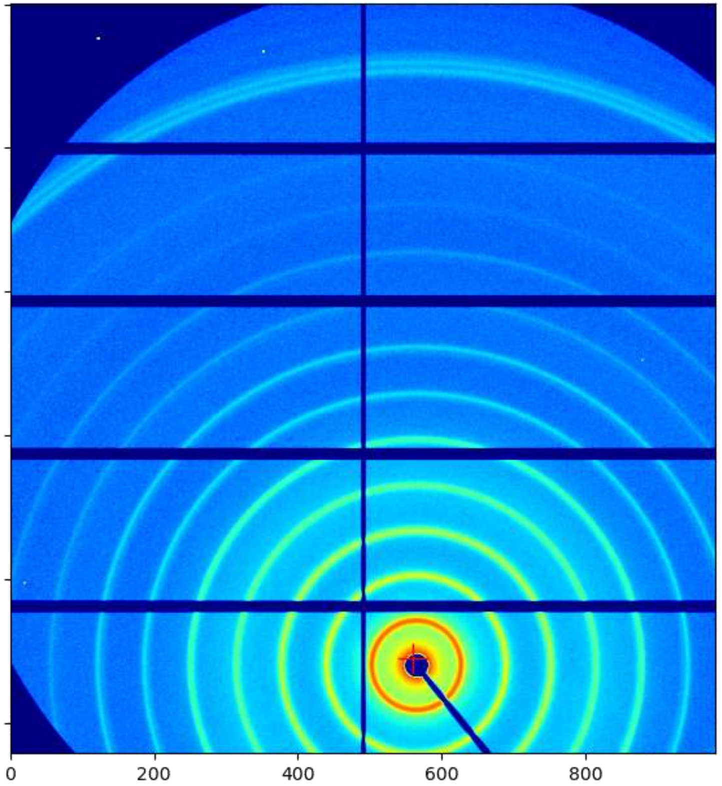

T=3600s
D=40cm

Tetradecanol

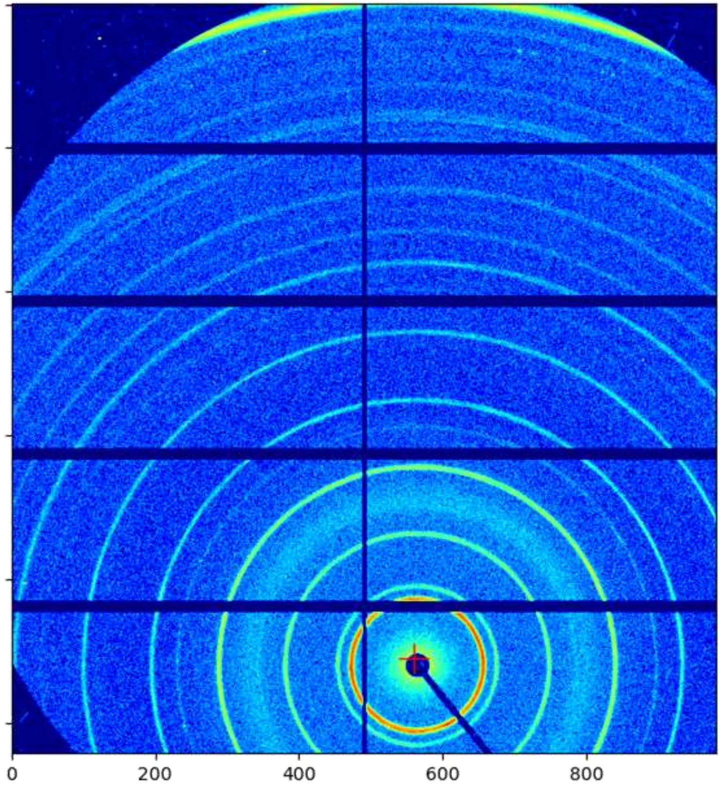

T=120s
D=40cm

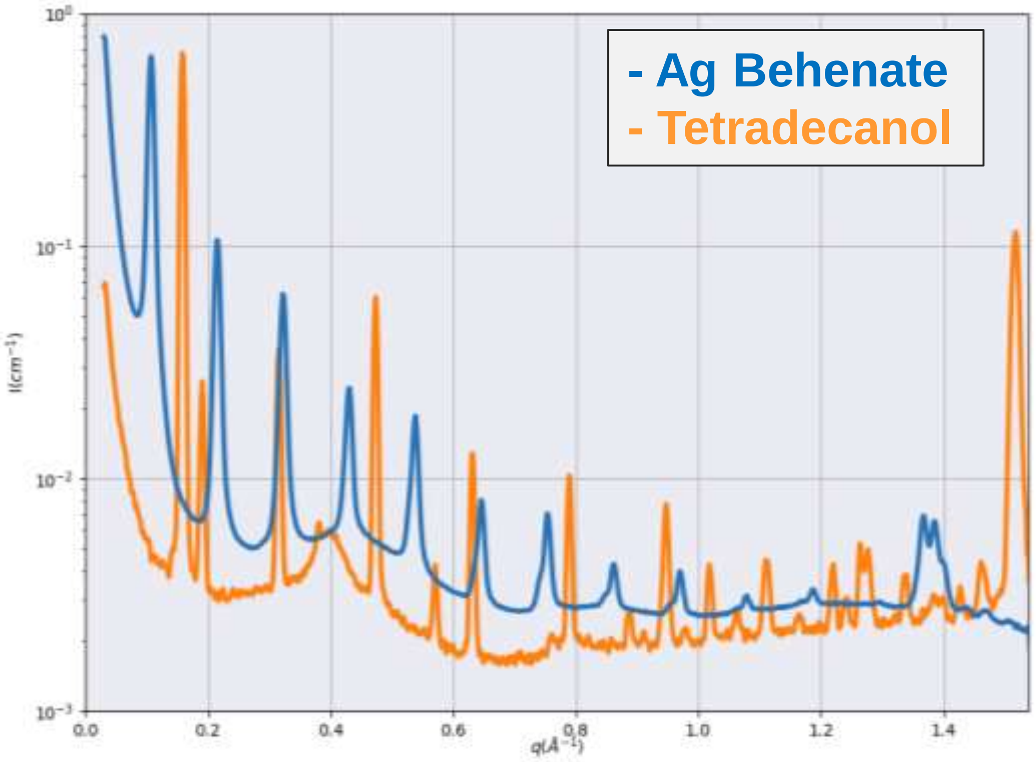

LLB Xeuss instrument

pyFAI

Search docs

- General introduction
- Example of usage
- Application manuals
- Design of the library
- Python programming API

Docs » Fast Azimuthal Integration using Python   View page source

Fast Azimuthal Integration using Python

PyFAI is a python libary for azimuthal integration of X-ray/neutron/electron scattering data acquired with area detectors. For this, images needs to be re-binned in polar coordinate systems. Additional tools are provided to calibrate the experimental setup, i.e. define where the detector is positioned in space considering the sample and the incident beam.

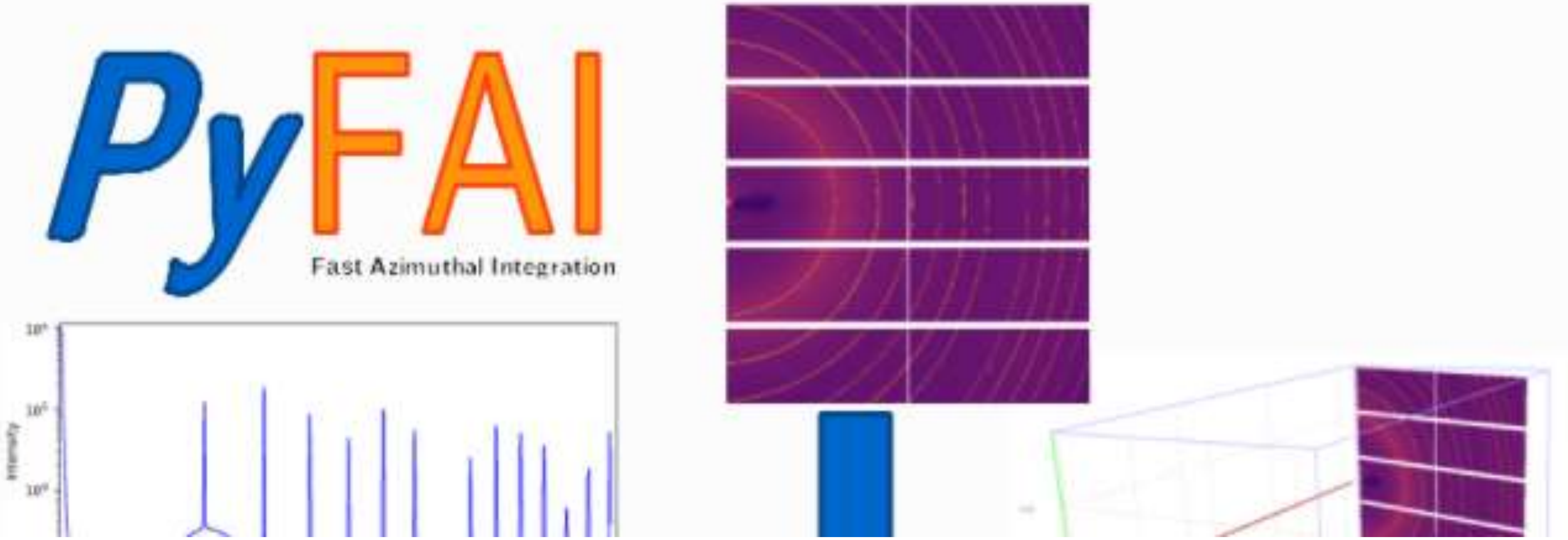

ESRF
The European Synchrotron

Publications about pyFAI

- *PyFAI, a versatile library for azimuthal regrouping*, J Kieffer & D Karkoulis; **Journal of Physics: Conference Series** (2013) 425 (20), pp202012 Initial publication where the usage of GPU is envisaged to overcome the speed limitation of azimuthal integration.
- *PyFAI: a Python library for high performance azimuthal integration on GPU* J Kieffer & J.P. Wright; **Powder Diffraction** (2013) 28 (S2), pp339-350 Introduces the concept of look-up table to register the pixel distribution
- ***PyFAI: a Python library for high performance azimuthal integration on GPU***;

  Jérôme Kieffer, Giannis Ashiotis **PROC. OF THE 7th EUR. CONF. ON PYTHON IN SCIENCE** (EUROSCIPY 2014) Presents the usage of sparse matrices to store the look-up table

Detector position

In pyFAI, the experiment geometry is defined by the position of the detector in space, the origin being located at the sample position, more precisely where the X-ray beam crosses the diffractometer main axis.

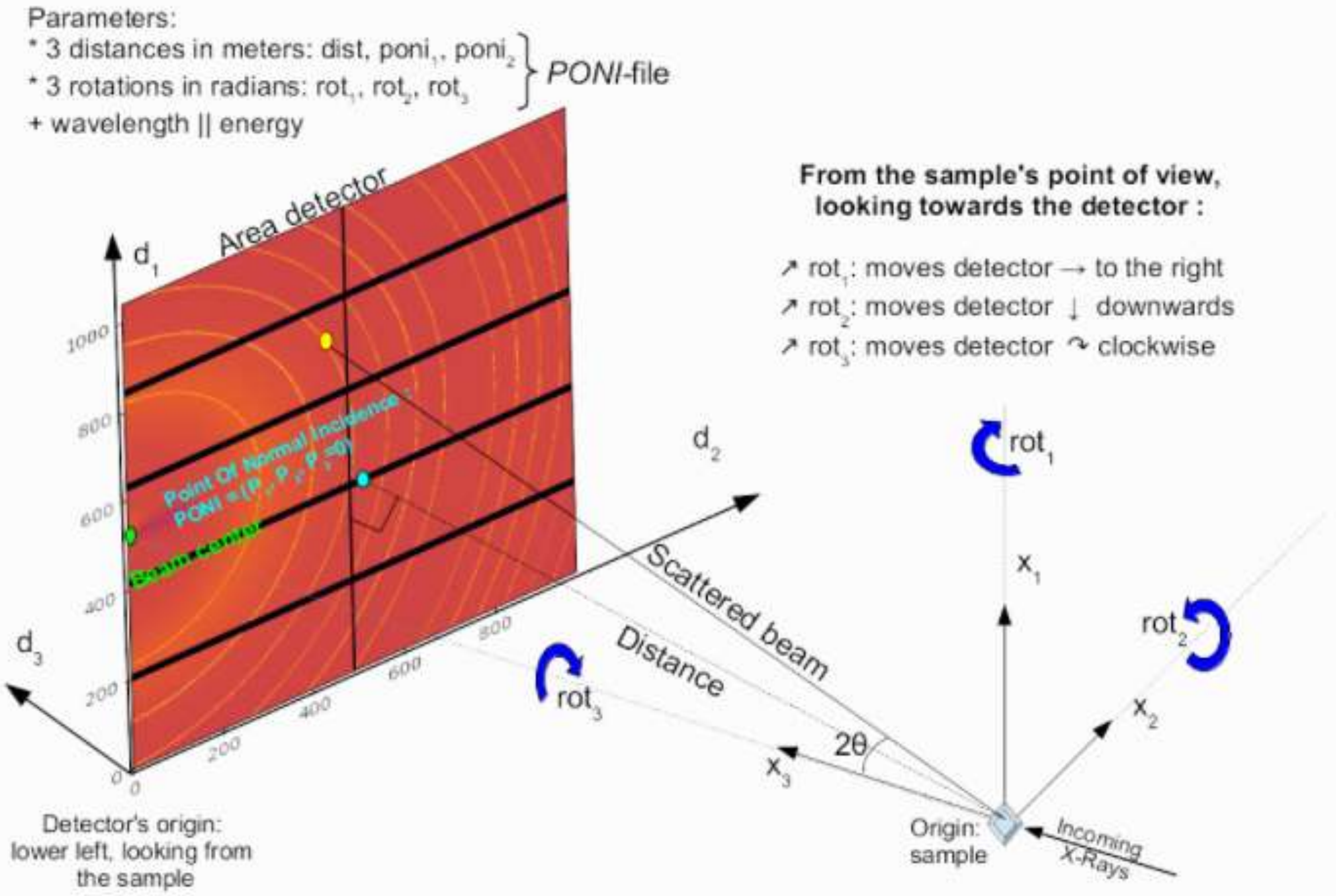

Demonstration

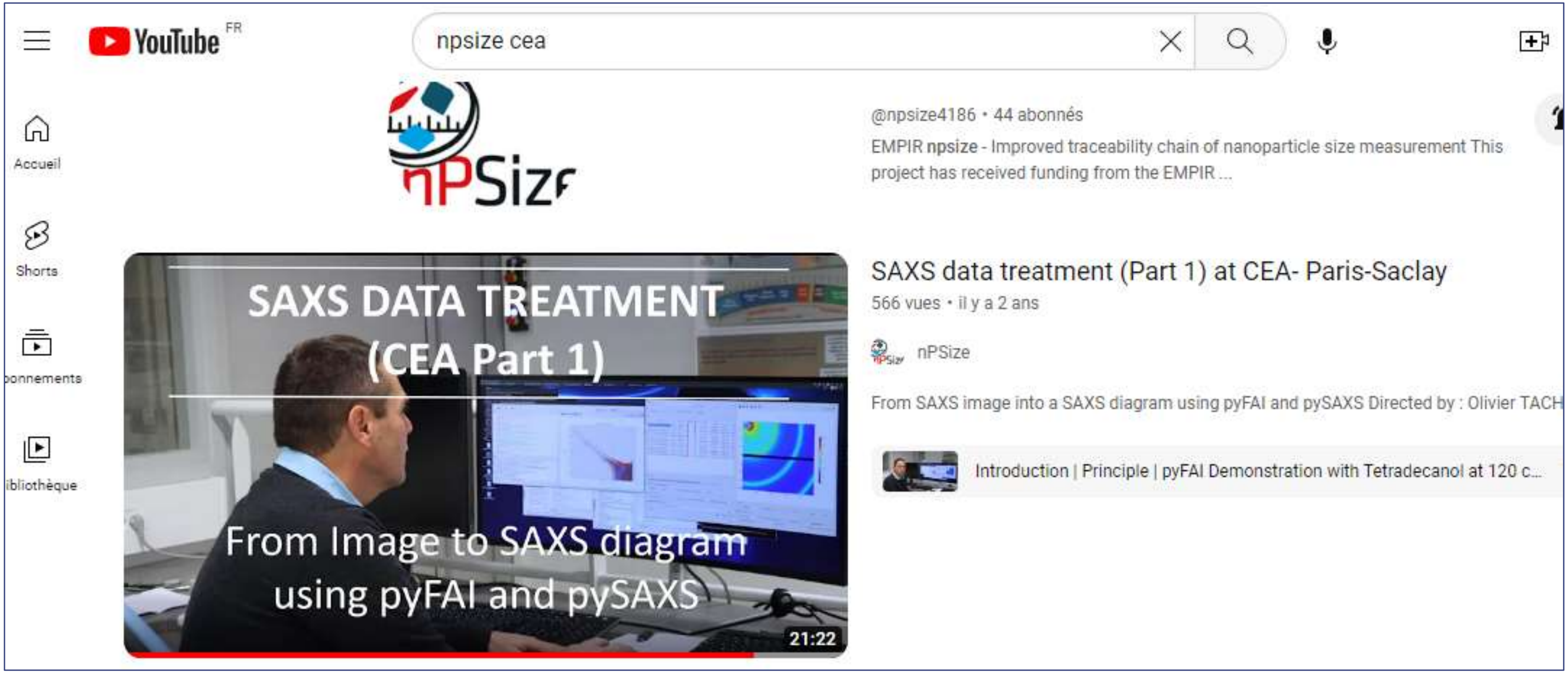

DATA TREATMENT

INTENSITIES CALIBRATIONS

Calculation of the absolute X-ray scattering intensities

The absolute X-ray scattering intensity is a measure of the **probability** that a photon will be scattered as it passes through a sample.

This quantity is directly related to the structure of the sample and can be used to determine various physical properties : molecular weight, particle number density, volume fraction, and specific surface area.

Number of counts detected

$$I(q) = \frac{d\Sigma}{d\Omega}(q) = \frac{\eta_{QE1}}{\eta_{QE2}} \cdot \frac{C_{ij} - darkcurrent}{\phi_{out}} \cdot \frac{1}{\Delta\Omega \cdot t_{exp} \cdot \omega}$$

Efficienty detectors constants

Integrated Transmitted Flux

$$\Delta\Omega = \left(\frac{s}{L}\right)^2$$

Sample thickness

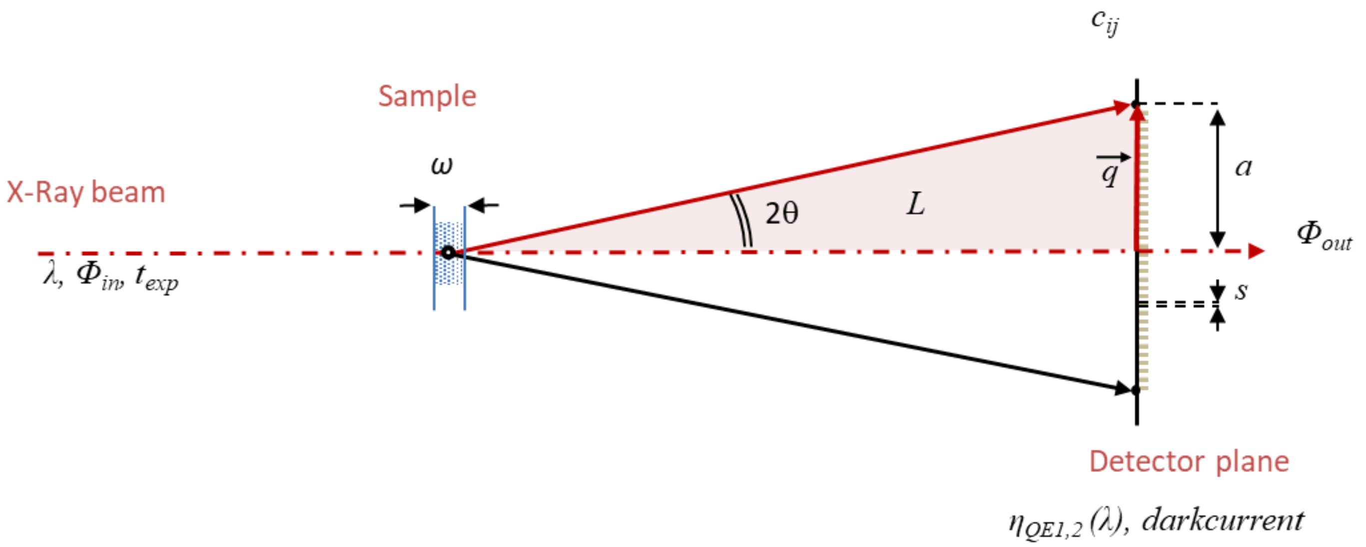

All SAXS experimental contributions are:

Contribution	DESCRIPTION	UNIT
Cij	Measured intensities at pixel i,j	photons
λ	Main wavelength	m
ϕ_{in}	Incident flux	photons
ϕ_{out}	Transmitted flux	photons
t_{exp}	Experiment time	s
ω	Sample Thickness	mm
L	Sample to detector distance	mm
A	Distance from beam center to q	mm
S	Pixel size	mm
η_{qe1}	Detector efficiency for ϕ_{out}	
η_{qe2}	Detector efficiency for Cij	
darkcurrent	Detector dark current	Photons/pixel
T	Transmission	

Calculation of the absolute X-ray scattering intensities

The absolute X-ray scattering intensity is a measure of the **probability that a photon** will be scattered as it passes through a sample.

This quantity is directly related to the structure of the sample and can be used to determine various physical properties : molecular weight, particle number density, volume fraction, and specific surface area.

Number of counts detected

$$I(q) = \frac{d\Sigma}{d\Omega}(q) = \frac{\eta_{QE1}}{\eta_{QE2}} \cdot \frac{C_{ij} - darkcurrent}{\phi_{out}} \cdot \frac{1}{\Delta\Omega \cdot t_{exp} \cdot \omega}$$

Efficiency detectors constants

Integrated Transmitted Flux

$$\Delta\Omega = \left(\frac{S}{L}\right)^2$$

Sample thickness

Main uncertainties for q

CONTRIBUTION	LABORATORY EST. STANDARD DEV (SMALES PAPER)	SYNCHROTRON EST. STANDARD DEV (SHAVKAN PAPER)
λ Wavelength	0.25 %	0.01 %
L Sample to detector distance	0.5 %	0.2 %
S pixel size	0.2 %	0.2 %
TOTAL	1 %	0.5 %

The uncertainty in *q* can be less than 1% for laboratory instruments and less than 0.5% for Synchrotron instruments.

Main uncertainties for Intensities (q)

CONTRIBUTION	LABORATORY EST. STANDARD DEV (SMALES PAPER)	SYNCHROTRON EST. STANDARD DEV (SHAVKAN PAPER)
Incident flux ϕ_{in}	0.071 %	1 %
Transmission	0.23 %	1 %
Solid angle ΔΩ	1 %	0.2 %
Sample thickness ω	1 %	3 %
TOTAL	2.3 %	5.2 %

The biggest uncertainties are derived from the determination of the sample thickness ω.

"Report on uncertainty statements for the nanoparticle concentration determination by SAXS" npSize 2021

Contributions from Glen Smales*, Brian Pauw*, Jerome Deumer**, Christian Gollwitzer**.
* *Bundesanstalt für Materialforschung und -prüfung, Unter den Eichen 44-46, 12203 Berlin, Germany*
***Physikalisch-Technische Bundesanstalt, Institut Berlin, Abbestr. 2, 10587 Berlin, Germany*

The EMPIR initiative is co-funded by the European Union's Horizon 2020 research and innovation programme and the EMPIR Participating States

Calculation of the absolute X-ray scattering intensities

The absolute X-ray scattering intensity is a measure of the **probability that a photon** will be scattered as it passes through a sample.

This quantity is directly related to the structure of the sample and can be used to determine various physical properties : molecular weight, particle number density, volume fraction, and specific surface area.

Number of counts detected

$$I(q) = \frac{d\Sigma}{d\Omega}(q) = \frac{\eta_{QE1}}{\eta_{QE2}} \cdot \frac{C_{ij} - darkcurrent}{\phi_{out}} \cdot \frac{1}{\Delta\Omega \cdot t_{exp} \cdot \omega}$$

Efficiency detectors constants

Integrated Transmitted Flux

$$\Delta\Omega = \left(\frac{s}{L}\right)^2$$

Sample thickness

There are two main approaches to determining the absolute X-ray scattering intensity:

Direct method:
This method use the direct beam and the scattering intensities measured by the same detector. Metrologicaly traceable
On modern laboratory sources : stable flux, high detector dynamic, accurate detector distance

Standard calibration method: This method compares the scattering intensity of the sample a calibration standard

Several materials can be used as calibration standards for X-ray scattering:
Glassy carbon: Glassy carbon is a strong and stable scatterer, making it a convenient secondary standard. Its absolute intensity must be previously measured on a primary calibration instrument, such as a USAXS synchrotron instrument.

Other standards: Other materials, such as silica suspensions, Lupolen, and calibrated foils, have also been used as secondary standards.

Water: Water is a primary standard because its scattering cross section can be calculated theoretically. However, it scatters weakly and requires long measurement times, especially with low-flux laboratory X-ray sources.

Reference Materials

JOURNAL OF APPLIED CRYSTALLOGRAPHY

ISSN 1600-5767

MOMAC: a SAXS/WAXS laboratory instrument dedicated to nanomaterials

Olivier Taché,[a] Stéphan Rouzière,[b] Philippe Joly,[b] Mohamed Amara,[b] Blaise Fleury,[a] Antoine Thill,[a] Pascale Launois,[b] Olivier Spalla[a] and Benjamin Abécassis[b]*

[a]LIONS, NIMBE, CEA, CNRS, Université Paris Saclay, CEA Saclay, 91191 Gif-sur-Yvette, France, and [b]Laboratoire de Physique des Solides, CNRS, Université Paris-Sud, Université Paris-Saclay, 91405 Orsay Cedex, France. *Correspondence e-mail: benjamin.abecassis@gmail.com

Received 19 April 2016
Accepted 26 July 2016

NIST Glassy Carbon 1mm

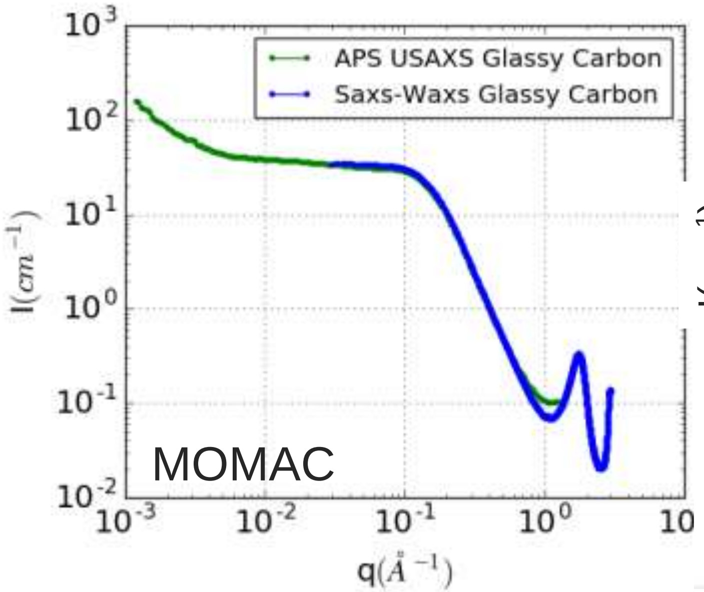

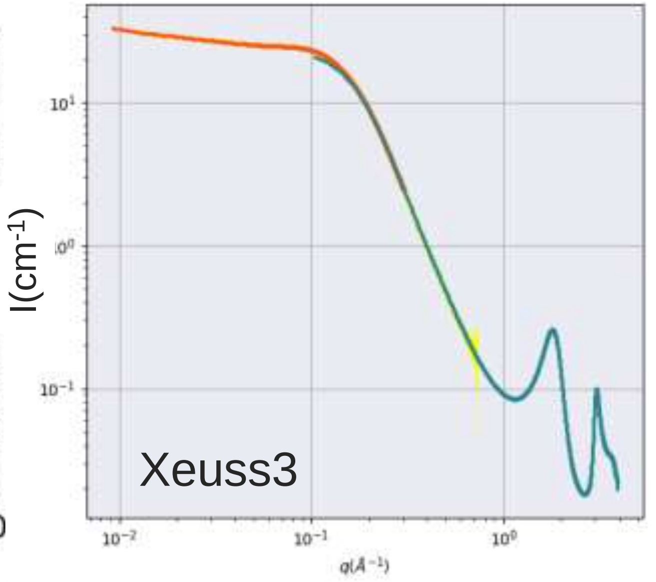

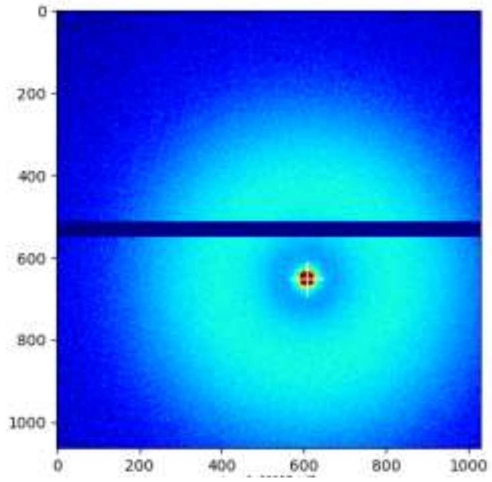

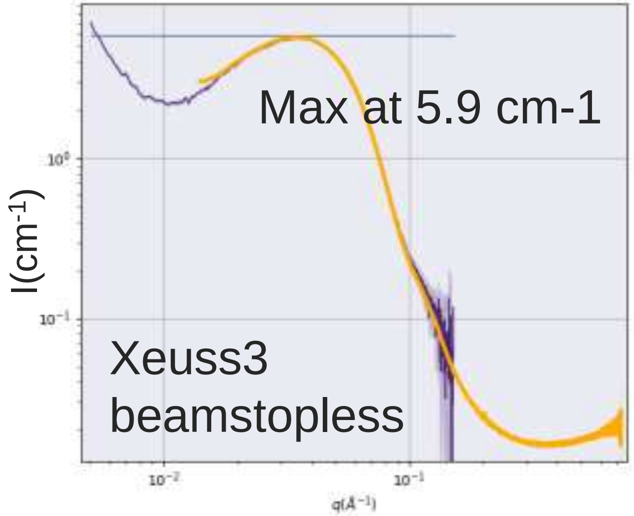

Maximum at 5.9 cm-1 certified by metrological beamline at PTB (2019)

JOURNAL OF APPLIED CRYSTALLOGRAPHY

ISSN 1600-5767

NIST Standard Reference Material 3600: Absolute Intensity Calibration Standard for Small-Angle X-ray Scattering

Andrew J. Allen,[a]* Fan Zhang,[a] R. Joseph Kline,[b] William F. Guthrie[c] and Jan Ilavsky[d]

J. Appl. Cryst. (1974). 7, 159

Calibration of Polyethylene (Lupolen) as a Wavelength-Independent Absolute Intensity Standard*

By Lawrence B. Shaffer† and Robert W. Hendricks
Metals and Ceramics Division, Oak Ridge National Laboratory, Oak Ridge, Tennessee 37830, U.S.A.

Calculation of the absolute X-ray scattering intensities

The absolute X-ray scattering intensity is a measure of the **probability that a photon** will be scattered as it passes through a sample.

This quantity is directly related to the structure of the sample and can be used to determine various physical properties : molecular weight, particle number density, volume fraction, and specific surface area.

Number of counts detected

$$5.9 = \frac{d\Sigma}{d\Omega}(q) = \frac{\eta_{QE1}}{\eta_{QE2}} \cdot \frac{C_{ij} - darkcurrent}{\phi_{out}} \cdot \frac{1}{\Delta\Omega \cdot t_{exp} \cdot \omega}$$

Integrated Transmitted Flux

$$\Delta\Omega = \left(\frac{s}{L}\right)^2$$

Sample thickness

This constant gives the ratio measured cp/s and measured ϕ_{out}

$Tr = \phi_{in} / \phi_{out}$ this method can determine ϕ_{in}

There are two main approaches to determining the absolute X-ray scattering intensity:

Direct method:
This method use the direct beam and the scattering intensities measured by the same detector. Metrologicaly traceable

Standard calibration method: This method compares the scattering intensity of the sample a calibration standard

LUPOLEN

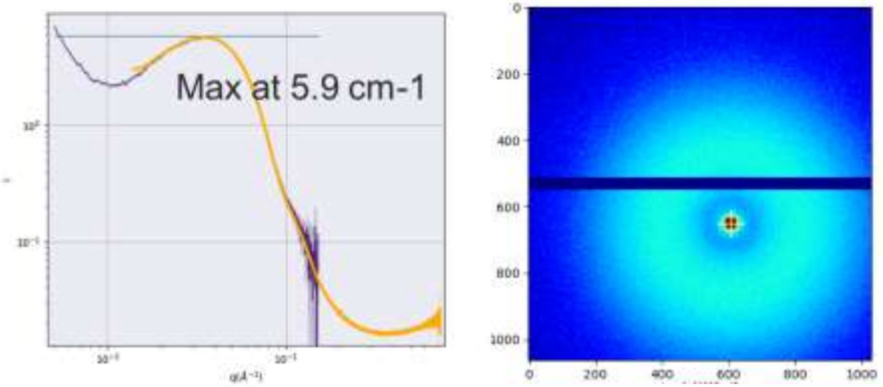

Absolute intensities

Absolute intensities

- For size measurements only angles need to be traceable
- For concentration Intensity also need to be traceable

Ne, F., I. Grillo, O. Tache, et T. Zemb. « From raw image to absolute intensity: Calibration of a Guinier-Mering camera with linear collimation ». *Journal De Physique Iv* 10, nº P10 (septembre 2000): 403-13.

Calibration samples:

- NIST glassy carbon
- Lupolen (polymer)

On modern laboratory instruments

- stable source
- scattered intensities and direct beam measured with the same detector
- Accurate distance estimation

Number of counts detected

$$5.9 = \frac{d\Sigma}{d\Omega}(q) = \frac{\eta_{QE1}}{\eta_{QE2}} \cdot \frac{C_{ij} - darkcurrent}{\phi_{out}} \cdot \frac{1}{\Delta\Omega \cdot t_{exp} \cdot \omega}$$

Efficienty detectors

Integrated Transmitted Flux need to be measured

Sample thickness ~3mm

Internal background : coherent scattering

$$I = \rho\, b^2\; S(0)$$

Number of molecules per unit volume

Scattering length of a molecule

$$S(0) = \rho kT\, \chi_T$$

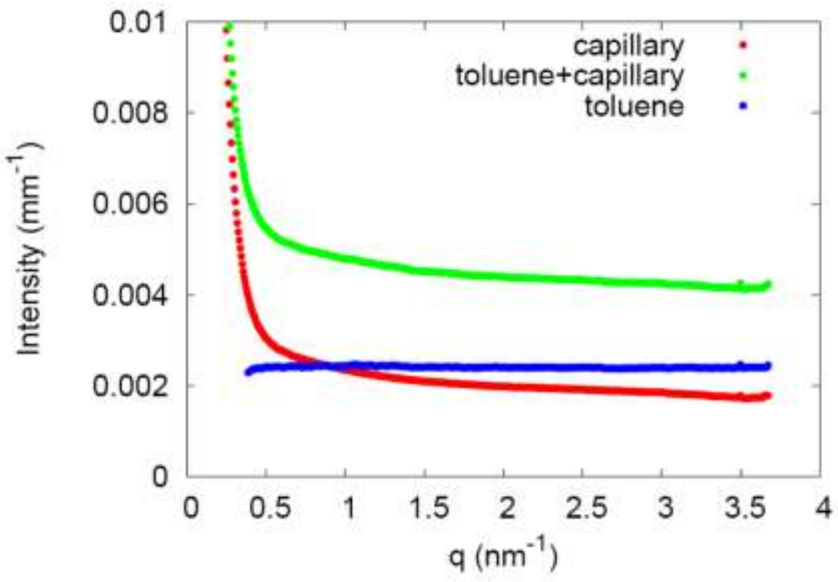

$$I = \rho^2\; b^2\; kT\, \chi_T$$

Solvent	ρ $(molecules/cm^3)$	$b(cm)$	$\chi_T\ (Pa^{-1})$	$I(cm^{-1})$
water	$3.3\ 10^{22}$	$2.82\ 10^{-12}$	$4.57\ 10^{-10}$	**0.0162 (25°C)**

Hexane I = *0.0287 cm^{-1}*

Toluene I = *0.0236 cm^{-1}*

ρ is the density of water.
k_B is the Boltzmann constant.
T is the temperature.
χ_T is the isothermal compressibility.

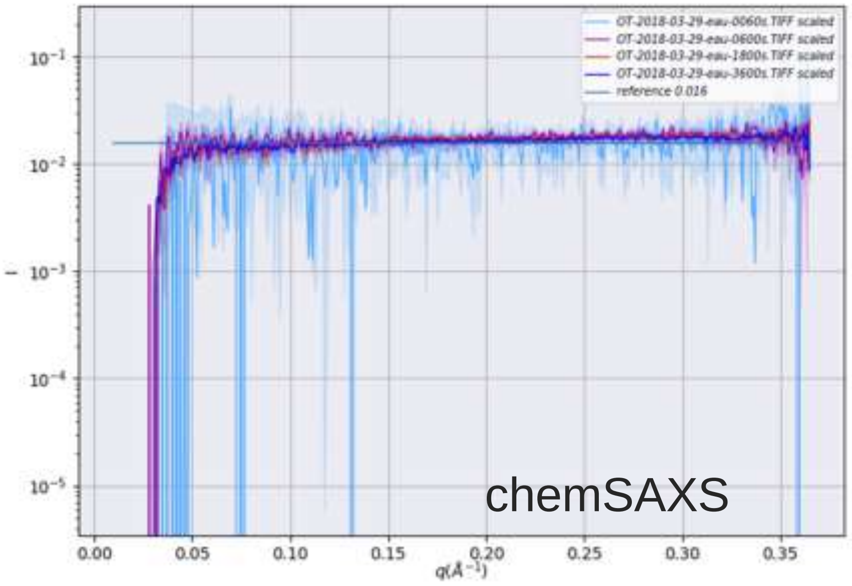

Calculation of the absolute intensity : solvent subtraction

What is measured ? :

T : transmission
E : thickness
N : number of counts in the detector
I : absolute intensities

EB : Electronic background

Total
$T = T_{EC}\, T_S$

$$\frac{\Delta N_{Tot}}{\Delta\Omega} = EB + T_{EC}\left(\frac{\Delta N_S}{\Delta\Omega} - EB\right) + T_S\left(\frac{\Delta N_{EC}}{\Delta\Omega} - EB\right)$$

Windows
T_{EC}

$$\frac{\Delta N_{EC}}{\Delta\Omega} = EB + N_0\, T_{EC}\, e_{EC}\, I_{EC}$$

Sample
$T_S\, e_S$

$$\frac{\Delta N_S}{\Delta\Omega} = EB + N_0\, T_S\, e_S\, I_S$$

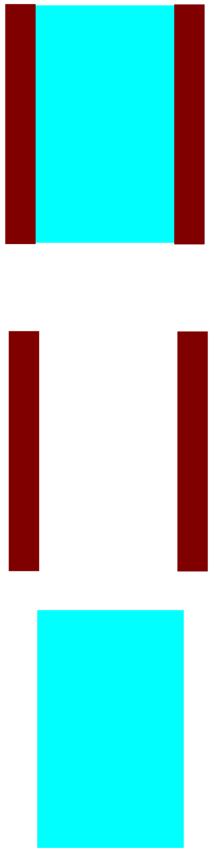

$$I_S = \frac{1}{N_0 e_S}\left[\frac{1}{T}\left(\frac{\Delta N_{Tot}}{\Delta\Omega} - EB\right) - \frac{1}{T_{EC}}\left(\frac{\Delta N_{EC}}{\Delta\Omega} - EB\right)\right]$$

Capillary thickness estimation

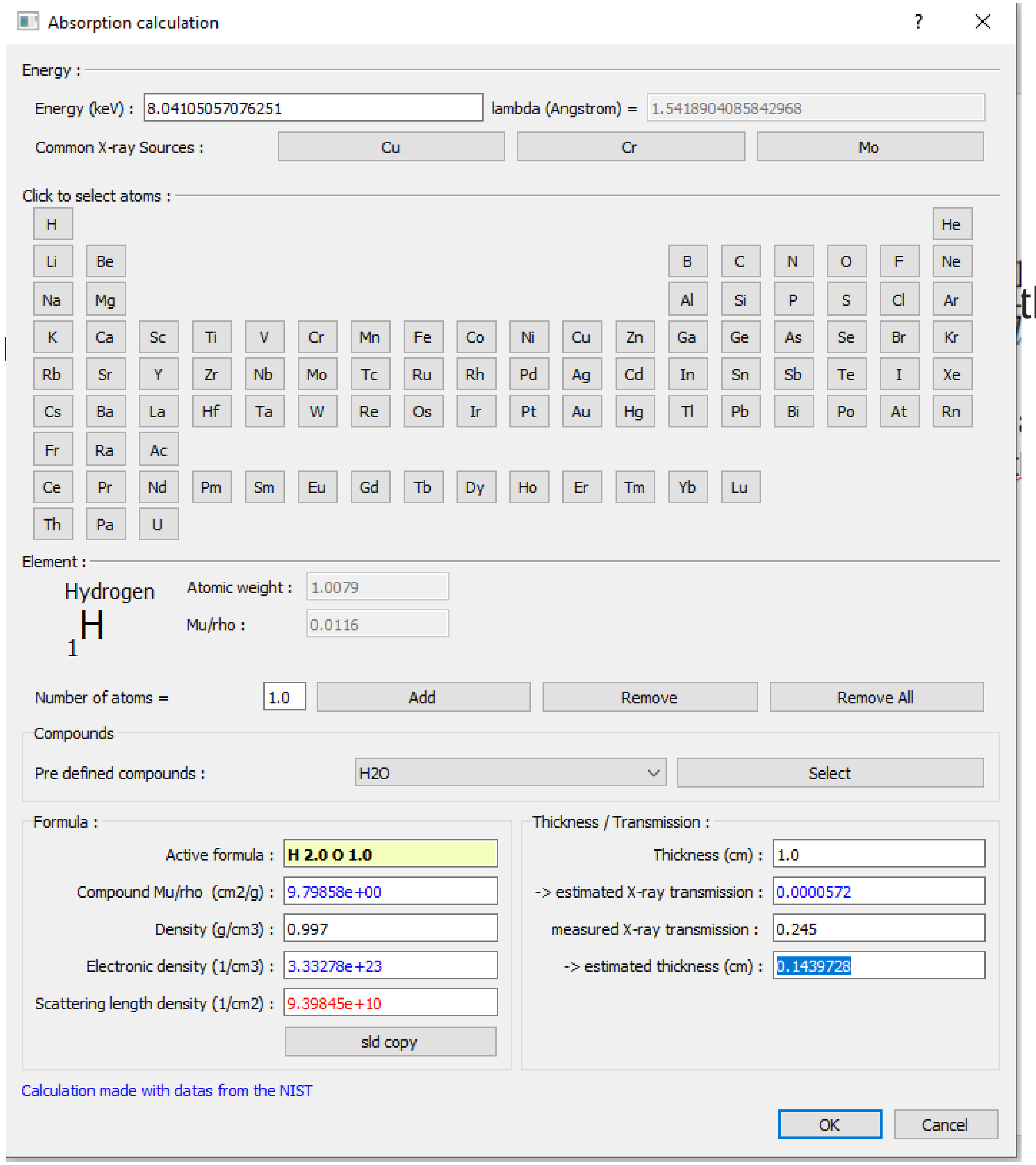

$$\bar{W} = \frac{1}{db}\int_{-db/2}^{db/2} 2\sqrt{R^2 - y^2}\, dy$$

If Dc=1.5 mm and the beam size is *db* = 0.8 mm, the mean width at the center is *W* = 1.43 mm

Thickness estimated by the water transmission using pySAXS

W=0.144

Capillary thickness estimation

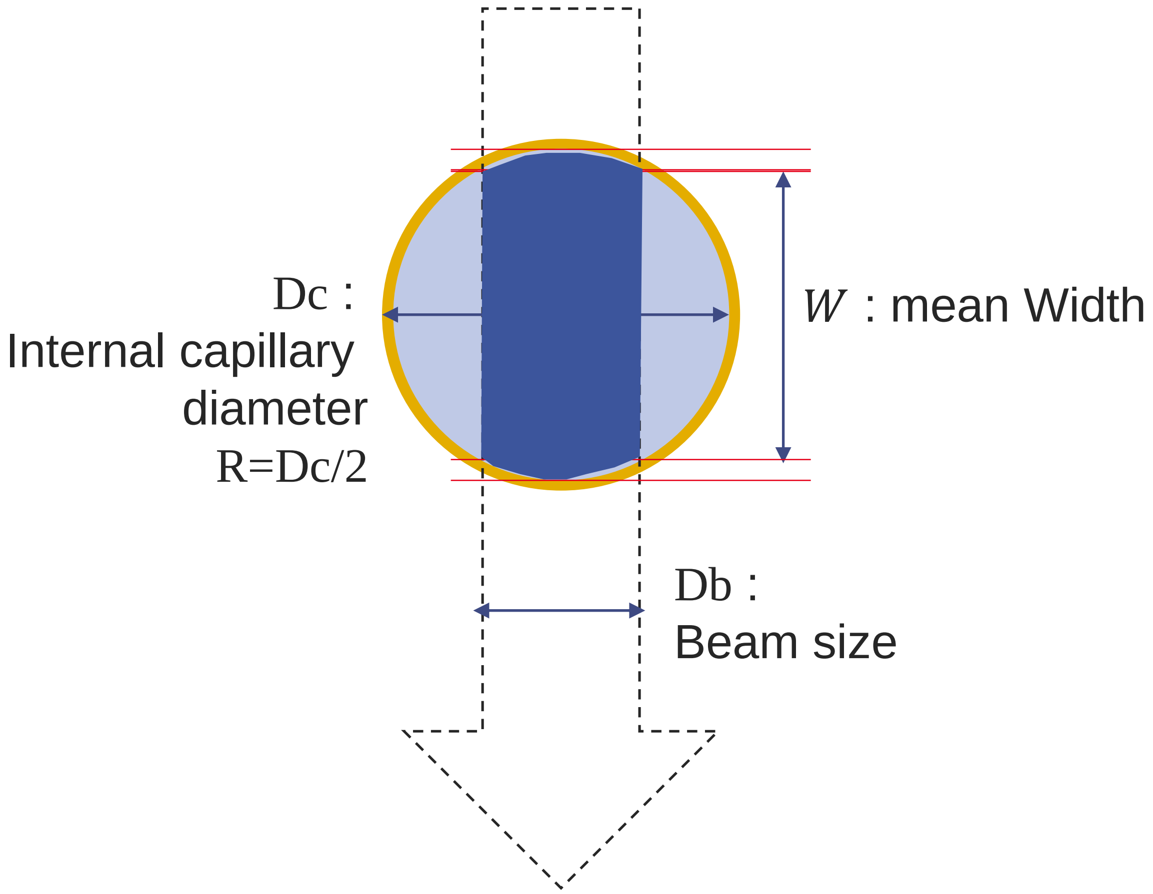

$\bar{W}$

If Dc=1.5 mm and the beam size is *db* = 0.8 mm, the mean width at the center is *W* = 1.43 mm

Calculation of the absolute intensity : solvent subtraction

What is measured ? :

T : transmission
E : thickness
N : number of counts in the detector
I : absolute intensities

EB : Electronic background

Total
$T = T_{EC}\, T_S$

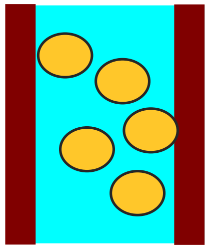

$$\frac{\Delta N_{Tot}}{\Delta\Omega} = EB + T_{EC}\left(\frac{\Delta N_S}{\Delta\Omega} - EB\right) + T_S\left(\frac{\Delta N_{EC}}{\Delta\Omega} - EB\right)$$

Windows
T_{EC}

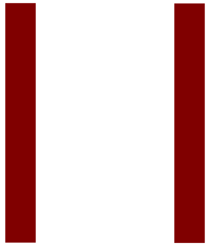

$$\frac{\Delta N_{EC}}{\Delta\Omega} = EB + N_0\, T_{EC}\, e_{EC}\, I_{EC}$$

Sample
$T_S\, e_S$

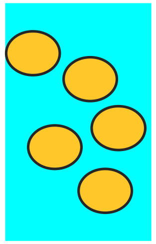

$$\frac{\Delta N_S}{\Delta\Omega} = EB + N_0\, T_S\, e_S\, I_S$$

$$I_S = \frac{1}{N_0 e_S}\left[\frac{1}{T}\left(\frac{\Delta N_{Tot}}{\Delta\Omega} - EB\right) - \frac{1}{T_{EC}}\left(\frac{\Delta N_{EC}}{\Delta\Omega} - EB\right)\right]$$

$$I_{part} = I_{total} - (1 - volumic\ fraction) \times I_{solv}$$

SAXS experimental contribution and uncertainties for concentration

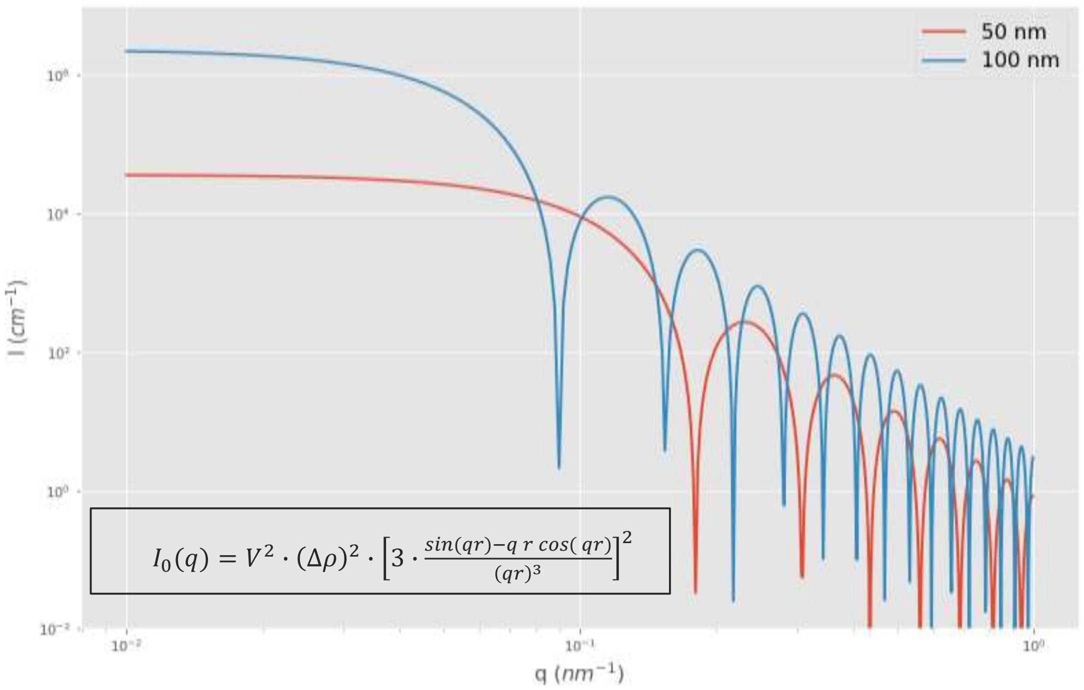

$$I_0(q) = V^2 \cdot (\Delta\rho)^2 \cdot \left[3 \cdot \frac{\sin(qr) - q\,r\cos(qr)}{(qr)^3}\right]^2$$

The scattering intensity I(q) of a number n of spherical particles, equals of the sum of the intensities I_0 of same size single particles: $I(q) = n \cdot I_0$

n is the concentration of sphere (number / cm-3)

Then, if dΣ/dΩ (usually scaling in 1/cm or 1/m) is known, the number concentration n of the suspended particle ensemble can be determined.

The second type of contributions comes from the nanoparticles suspension themselves. We can extract the main parameters from equation (6). The radius of the particle *r* can be estimated from the signal oscillations in q with a very high accuracy. *ρ* strictly depends on the density of the elements. The atomic composition used for the calculation of the Scattering Length Density is assumed to be known to a high degree of accuracy, though literature values shows a large span of range.

CONTRIBUTION	DESCRIPTION	UNIT	EST. STANDARD DEV	DETERMINED BY :
r	Radius of the particle	Å	1 %	Q uncertainties
ρ	Density of particles	g/cm³	5 %	Known atomic composition (Smales paper)
TOTAL			6 %	

The total uncertainty contributions in intensity is in the range of 8% to 11% depending the sample thickness determination protocol and the density determination of the nanoparticles.

"Report on uncertainty statements for the nanoparticle concentration determination by SAXS" npSize 2021

Contributions from Glen Smales*, Brian Pauw*, Jerome Deumer**, Christian Gollwitzer**.
** Bundesanstalt für Materialforschung und -prüfung, Unter den Eichen 44-46, 12203 Berlin, Germany*
***Physikalisch-Technische Bundesanstalt, Institut Berlin, Abbestr. 2, 10587 Berlin, Germany*

cea

Demonstration of absolute intensities scaling

XEUSS 3 :

SAXS1 (detector to sample distance is 37 cm)

SAXS2 (detector to sample distance is 80 cm)

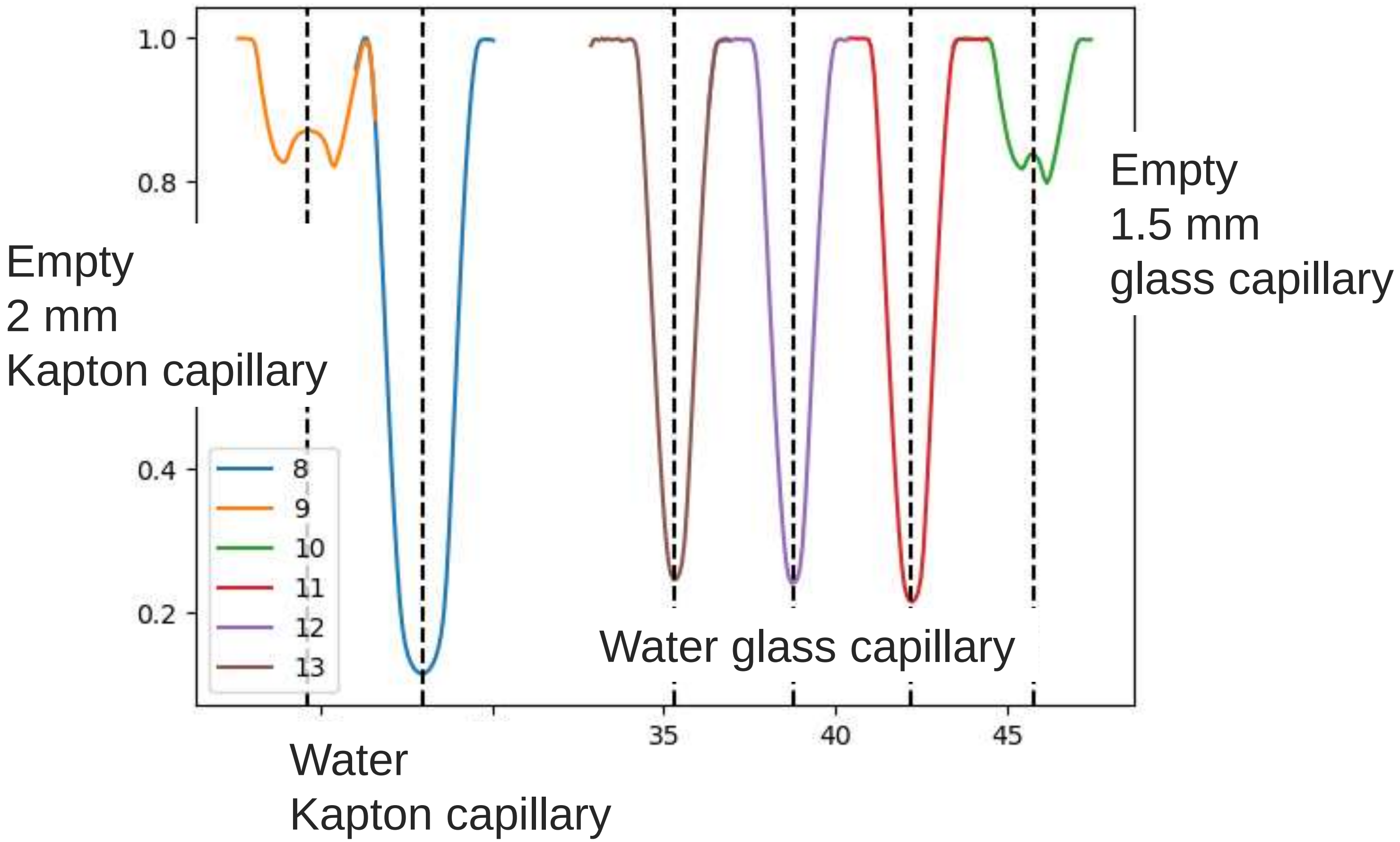

Why we developped a dedicated SAXS software ?
you need to manage different kind of saxs datas
manage the uncertainties

DATA TREATMENT

Conclusion

SAXS Reproducibility

Comparison of instruments

Same sample (NPSIZE10),
Same user (O. TACHE)
Sample reprepared
Different instruments (DIAMOND, PTB, XEUSS2, XEUSS3, chemSAXS)
Same software

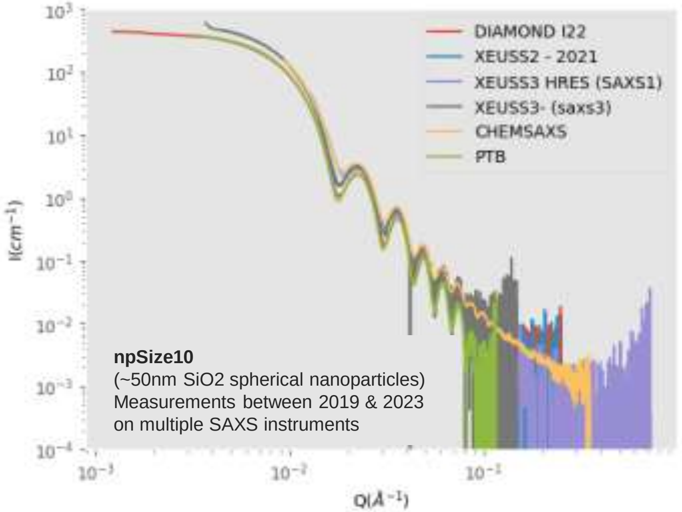

Comparison of laboratories

Same sample,
Different users
Sample reprepared
Different instruments (28)
Same softwares

JAC JOURNAL OF APPLIED CRYSTALLOGRAPHY
ISSN 1600-5767

Nanoparticle size distribution quantification: results of a small-angle X-ray scattering inter-laboratory comparison

Brian R. Pauw,* Claudia Kästner and Andreas F. Thünemann*

Received 28 March 2017
Accepted 7 July 2017

Federal Institute for Materials Research and Testing (BAM), Unter den Eichen 87, 12205 Berlin, Germany. *Correspondence e-mail: brian.pauw@bam.de, andreas.thuenemann@bam.de

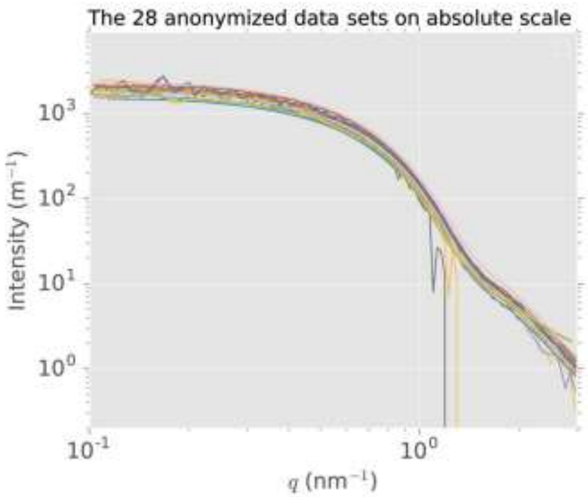

Comparison of analysis process

Same sample,
One instrument (PTB)
Different softwares

JAC JOURNAL OF APPLIED CRYSTALLOGRAPHY
ISSN 1600-5767

The human factor: results of a small-angle scattering data analysis round robin

Brian R. Pauw,[a*] Glen J. Smales,[a] Andy S. Anker,[b] Venkatasamy Annadurai,[c] Daniel M. Balazs,[d] Ralf Bienert,[e] Wim G. Bouwman,[f] Ingo Breßler,[a] Joachim Breternitz,[g] Erik S. Brok,[h] Gary Bryant,[i] Andrew J. Clulow,[j] Erin R. Crater,[k] Frédéric De Geuser,[l] Alessandra Del Giudice,[m] Jérôme Deumer,[n] Sabrina Disch,[o,p] Shankar Dutt,[q] Kilian Frank,[r] Emiliano Fratini,[s] Paulo R. A. F. Garcia,[t] Elliot P. Gilbert,[u] Marc B. Hahn,[a] James Hallett,[v] Max Hohenschutz,[w] Martin Hollamby,[x] Steven Huband,[y] Jan Ilavsky,[z] Johanna K. Jochum,[aa] Mikkel Juelsholt,[bb] Bradley W. Mansel,[cc] Paavo Penttilä,[dd] Rebecca K. Pittkowski,[b] Giuseppe Portale,[ee] Lilo D. Pozzo,[ff] Leonhard Rochels,[o,p] Julian M. Rosalie,[a] Patrick E. J. Saloga,[gg] Susanne Seibt,[j] Andrew J. Smith,[hh] Gregory N. Smith,[ii] Glenn A. Spiering,[jj] Tomasz M. Stawski,[ff] Olivier Taché,[kk] Andreas F. Thünemann,[a] Kristof Toth,[ll] Andrew E. Whitten[u] and Joachim Wuttke[mm]

Received 23 June 2023
Accepted 21 September 2023

Edited by T. J. Sato, Tohoku University, Japan

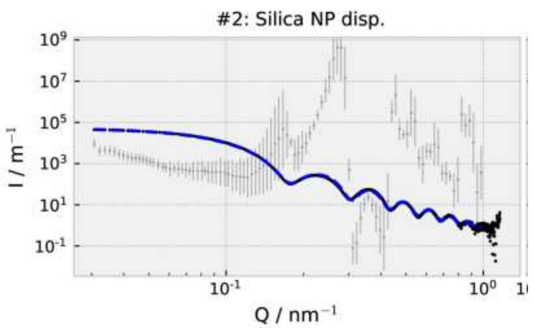

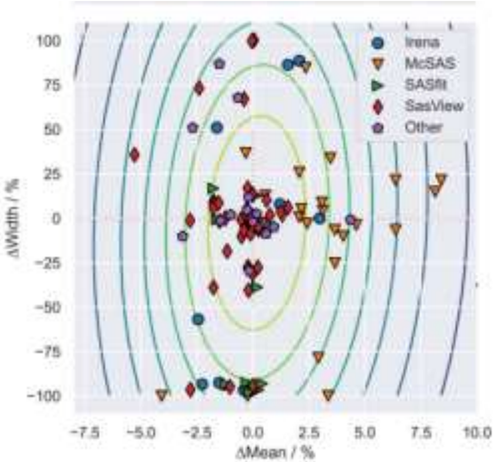

Acknowledgements

nPSize

EMPIR EURAMET

The EMPIR initiative is co-funded by the European Union's Horizon 2020 research and innovation programme and the EMPIR Participating States

This project has received funding from the EMPIR programme co-financed by the Participating States and from the European Union’s Horizon 2020 research and innovation Programme.

Lucien CEREJA,
Benedicte DURAND,
Aurely ARAMINTHE,
Kenza CHERGUI,
Aude HENRY,
Jean DUPRAT,

Fabienne TESTARD
Sylvie MARGUET
Antoine THILL
Elodie BARRUET
Frederic GOBEAUX
Valérie GEERTSEN
Mark LEVENSTEIN

cea